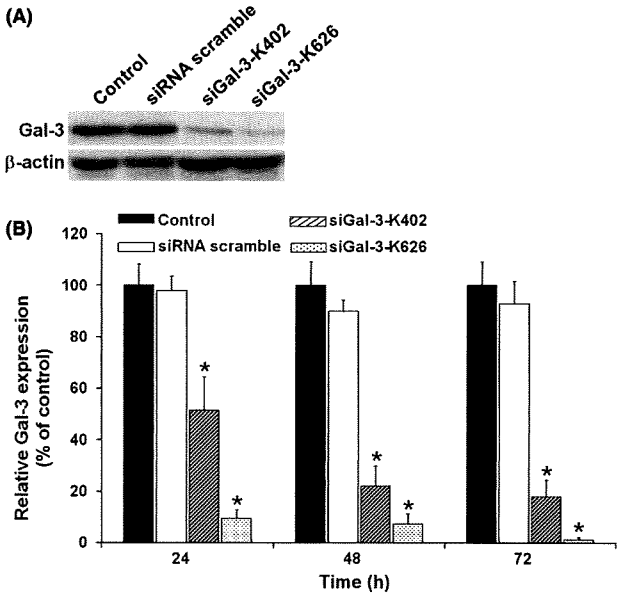

Fig. 1. Galectin-3 (Gal-3) suppression by siGal-3. Cholangiocarcinoma (CCA) cell line KKU-100 cells were transfected with siGal-3-K626 or siGal-3-K402 or siRNA-scramble using Lipofectamine 2000. (A) Expression of Gal-3 protein by immunoblotting with anti-Gal-3 after siGal-3 transfection for 72 h. (B) Relative Gal-3 expression levels (% of control) after siGal-3 transfection for 24 h, 48 h, and 72 h. Results are the mean ± SE (bars) of three independent experiments. $*P < 0.05$ compared with control cells.

cells underwent 70% apoptotic cell death, whereas only 5% of apoptotic cells were detected in the Gal-3 expressing cells ($P < 0.05$) (Fig. 2C).

Suppression of Gal-3 enhanced hypoxia and UV induced apoptosis. To demonstrate the anti-apoptotic role of Gal-3, CCA cell lines KKU-100 and KKU-M214, with or without transfection of siGal-3-K402, were induced to apoptosis by hypoxic conditions or UV irradiation. Compared to the parental control and siRNA-scramble-treated cells, the exposure of siGal-3-K402-treated cells to hypoxic conditions for 48 h resulted in significantly more apoptotic cells: 82.1 ± 0.58% and 65.5 ± 1.2% for KKU-100 and KKU-M214, respectively ($P < 0.05$) (Fig. 3A). Similarly, a short UV irradiation induced apoptosis in siGal-3-treated cells more than it did in the controls ($P < 0.05$). Exposure of CCA cells to UV caused an increase of 29.4 ± 2.6% and 13.9 ± 1.2% in apoptotic cells in siGal-3-K402-treated KKU-100 and KKU-M214, respectively (Fig. 3B). These results suggest a common role for Gal-3 in the anti-apoptotic process, regardless of the apoptotic inducer.

To investigate whether constitutive Gal-3 expression in CCA cells affected resistance to apoptotic stress, the anti-apoptotic activity of three CCA cell lines with different levels of Gal-3 expression, KKU-100 (high), KKU-OCA17 (moderate), and KKU-M055 (low), were examined under hypoxic conditions or UV irradiation. As shown in Figure 3(C), when comparing the corresponding control cells without apoptotic induction, the exposure of CCA cells to hypoxic conditions resulted in apoptosis of 74.3 ± 1.4% in KKU-100, 85.3 ± 0.8% in OCA17, and 89.9 ± 0.8% in KKU-M055. Similarly, the exposure of CCA cells to UV radiation induced apoptosis of 46.2 ± 5.2% in KKU-100, 88.9 ± 3.9% in OCA17, and 73.4 ± 2.5% in KKU-M055. These data reveal an important role of Gal-3 in regulating cell responses to apoptotic insults. The anti-apoptotic activity corresponded to the level of endogenous Gal-3 expression: the higher the level of endogenous Gal-3 expression, the higher the anti-apoptotic activity.

To ensure that UV irradiation did not alter Gal-3 expression, endogenous Gal-3 protein levels in KKU-100, KKU-OCA17, and KKU-M055 cells were determined 48 h after UV exposure. As shown in Figure 3(D), the levels of Gal-3 expression in all cell lines were not varied after UV irradiation; hence the anti-apoptotic response was based on the endogenous Gal-3.

Overexpression of Gal-3 rescued cells from apoptosis. To reveal the contribution of Gal-3 to anti-apoptosis, we next constructed an overexpressed Gal-3 CCA cell line using GFP expression vector pEGFP-C1-hGal3. KKU-M055, which had a low level of endogenous Gal-3, was transfected with pEGFP-C1-hGal3 or the control vector (pEGFP-C1), as controls. GFP-expressing cells observed by phase-contrast and fluorescence microscopy are shown in Figure 4(Aa,b). Transfection of

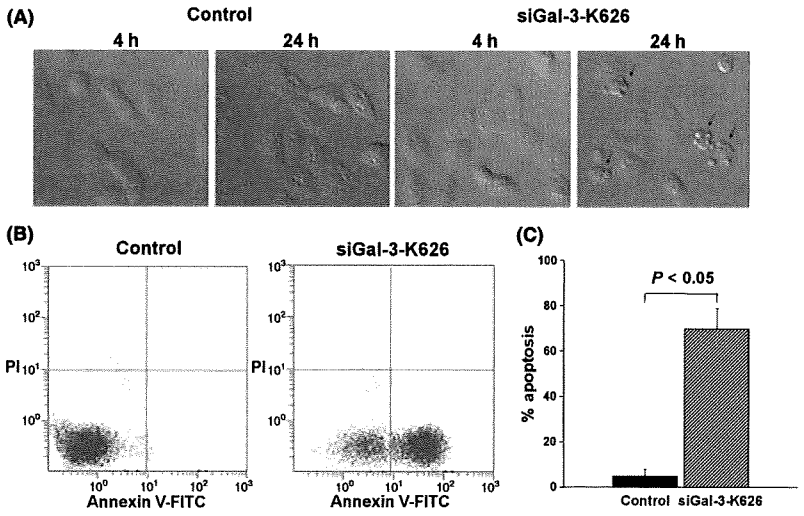

Fig. 2. Induction of apoptosis in cholangiocarcinoma (CCA) cell lines treated with siGal-3-K626. (A) Cell morphology of control and siGal-3-K626-treated cells was observed by time-lapse microscopy at 4 h and 24 h after transfection. (B) Apoptotic cells were detected in siGal-3-K626-treated cells using Annexin V and PI (propidium iodide) staining followed by flow cytometry. (C) The percentages of apoptotic cells were compared between siGal-3-K626-treated cells and controls. Results are the mean ± SE of three independent experiments.

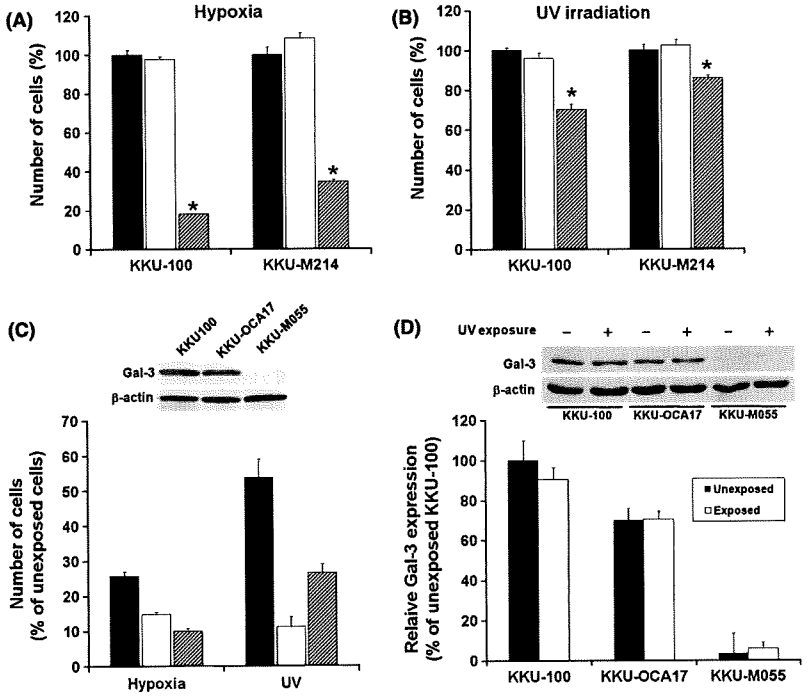

Fig. 3. siGal-3-K402 enhanced apoptosis in cholangiocarcinoma (CCA) cells under hypoxia and UV-induced apoptosis. CCA cell lines KKU-100 or KKU-M214 were treated with siRNA-scramble or siGal-3-K402 for 24 h, then grown (A) under hypoxic conditions for 48 h or (B) briefly exposed to UV radiation, then incubated at 37°C and 5% CO_2 for 48 h. The cell numbers were determined by sulforhodamine-B (SRB) assay thereafter: siGal-3-K402-treated cells (slash bar), parental cells (black bar), and siRNA-scramble cells (white bar). (C) Effects of hypoxia and UV-induced apoptosis on CCA cell lines with different endogenous galectin-3 (Gal-3) expressions: KKU-100 (high expression, black bar), KKU-OCA17 (moderate expression, white bar), and KKU-M055 (low expression, slash bar). (D) Endogenous Gal-3 expression of CCA cell lines after a short UV irradiation and culture for a further 48 h. Expressions of Gal-3 in KKU-100, KKU-OCA17, and KKU-M055 were determined by immunobloting (upper inset) and relative Gal-3 expression level (% of unexposed KKU-100) between UV-unexposed cells (black bar) and UV-exposed cells (white bar) were compared. Results are the mean ± SE of three independent experiments. *$P < 0.05$.

KKU-M055 cells with pEGFP-C1-hGal3 GFP vector resulted in 50–60% of GFP-labeled cells. The efficiency of transfection was monitored via GFP expressing cells. Approximately 50–60% of KKU-M055 cells were transfected with pEGFP-C1-hGal3. Moreover, cytofluorescence staining indicated that GFP-Gal-3 expressed in pEGFP-C1-hGal3-transfected cells could function in a similar manner to endogenous Gal-3 observed in KKU-100 cells. GFP-Gal-3 was found predominantly in the nucleus (Fig. 4Ac,d,g–h), and it translocated from the nucleus to the cytoplasm under apoptotic insult (Fig. 4Ai,j), as it did in KKU-100 cells (Fig. 4 Ae,f). The overexpression of Gal-3 protein was confirmed by Western blot analysis (Fig. 4B). Gal-3 expression in these cells was approximately 2.5-fold higher than the parental cells or pEGFP-C1-treated cells (Fig. 4C).

The anti-apoptotic role of Gal-3 in pEGFP-C1-hGal-3-transfected cells was compared with the parental (KKU-M055) cells and the control pEGFP-C1 vector–transfected cells, by culturing cells in hypoxic conditions or short term exposure to UV irradiation. As shown in Figure 4(E), hypoxic conditions or short UV exposure dramatically induced cell apoptosis of parental and control cells to <20% and 25% of the unexposed cells, respectively. Resistance to these apoptotic insults, however, was demonstrated in the Gal-3 overexpressing KKU-M055 cells. The numbers of pEGFP-C1-hGal3-transfected cells that remained in both apoptotic-induced conditions were significantly higher than those of the control cells ($P < 0.05$) (Fig. 4E).

Suppression of Gal-3 expression enhanced anticancer drug-induced apoptosis. To determine whether drug-induced apoptosis was enhanced by suppression of Gal-3 expression in CCA cell lines, siGal-3-K402 treated cells were cultured in the absence or presence of an anticancer drug for 48 h, and cell numbers were determined by the sulforhodamine-B (SRB) assay. Different concentrations of cisplatin at 4, 40, 400 μg/mL, and 5-FU at 1-1000 μg/mL for KKU-100 and 0.3–30 μg/mL for KKU-M214, were tested.

The chemotherapeutic drugs cisplatin and 5-FU induced apoptosis of CCA cells in a dose-dependent manner (Fig. 5A–D). Suppression of Gal-3 expression significantly enhanced drug-induced apoptosis in comparison with that of the control. Knockdown of Gal-3 expression in CCA cells significantly enhanced apoptosis induced by cisplatin at all concentrations tested ($P < 0.05$). Suppression of Gal-3 improved the action of cisplatin by approximately 10 times. Cells treated with siGal-3 or with a combination of 4 μM or 40 μM cisplatin reduced cell numbers to the same levels as cells treated with 40 μM or 400 μM cisplatin (Fig. 5A,C). Similar observations were obtained for cells treated with 5-FU (Fig. 5B,D). These results indicated that the RNAi-mediated knockdown of Gal-3 increased cell sensitivity to cisplatin- and 5-FU-induced apoptosis.

To examine whether or not the enhancement of apoptosis shown in anticancer-drug-treated Gal-3 knockdown cells was associated with Gal-3, Gal-3 overexpressing cells (pEGFP-C1-hGal3-transfected KKU-M055 cells) were treated with different concentrations of cisplatin (0.005, 0.05, 0.5 μg/mL) (Fig. 5E) and 5-FU (5, 50, 500 μg/mL) (Fig. 5F). Overexpression of Gal-3 significantly diminished the cisplatin- or 5-FU-induced apoptosis in KKU-M055 cells ($P < 0.05$).

doi: 10.1111/j.1349-7006.2009.01304.x

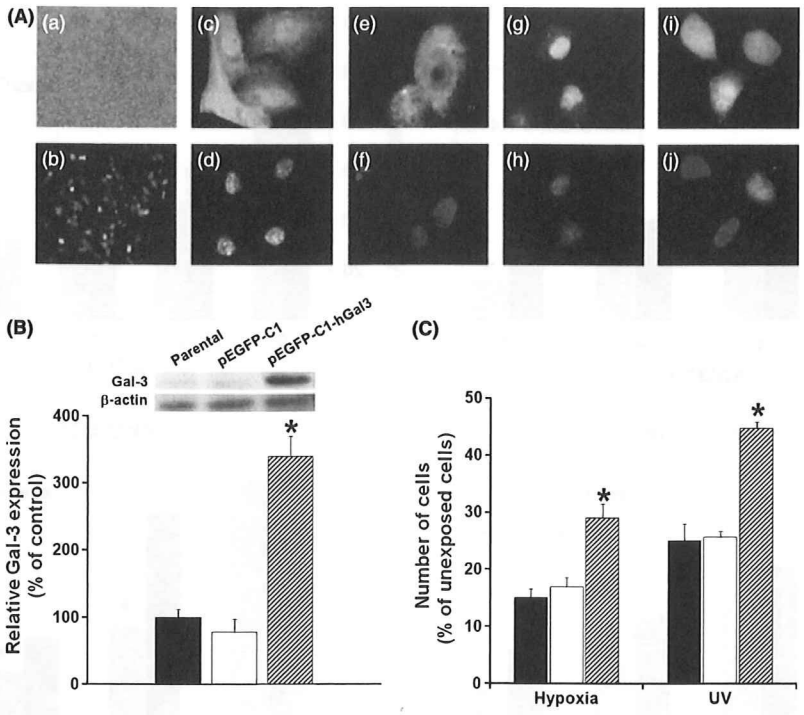

Fig. 4. The anti-apoptotic activity of galectin-3 (Gal-3) was demonstrated in Gal-3 overexpressing cells. The CCA cell line, KKU-M055, was transfected with the pEGFP-C1-hGal3 vector. The efficiency of the transfection was determined by (Aa) phase contrast, (Ab) GFP-fluorescence, and (B) relative expression of Gal-3 parental and vector pEGFP-C1-transfected cells determined by Western blotting of Gal-3. The function of GFP-Gal-3 was shown to be similar to the native Gal-3 of KKU-100; (Ac,e) immunofluorescence of Gal-3 in KKU-100; (Ag,i) immunofluorescence of GFP-Gal-3 in KKU-M055 transfected with pEGFP-C1-hGal3. (Ad,f,h,j) Hoechst 33342 staining for the nucleus. Endogenous Gal-3 was prominent in the nucleus (Ac,g) and translocated to the cytoplasm under siGal-3 treatment (Ad) or short UV exposure (Ai). (C) Effects of hypoxia and UV-induced apoptosis on KKU-M055 cells, as shown by comparing Gal-3 overexpressing cells with controls. Results are the mean ± SE of three independent experiments. $*P < 0.05$.

Discussion

Cholangiocarcinoma (CCA) is a fatal disease with poor prognosis and high recurrence. There is no effective treatment for CCA at present, probably due to its enhanced resistance to apoptosis. Accumulated evidence indicates that Gal-3 has anti-apoptotic effects in a variety of cells.[9–13] In this study, it was demonstrated that Gal-3 played a role in anti-apoptosis; reduction of Gal-3 expression significantly induced apoptosis in CCA cells and enhanced the responsiveness of CCA cells to chemotherapeutic agents.

The present study successfully established the RNA interference (RNAi)–mediated knockdown of Gal-3 and an overexpression system for Gal-3 in CCA cell lines. The anti-apoptotic activity of Gal-3 is dependent on the expression level of endogenous Gal-3. Apoptosis was dramatically induced in CCA cells in which Gal-3 expression was diminished to baseline levels with siGal-3-K626, whereas cells treated with siGal-3-K402 which suppressed Gal-3 expression to 50%, did not induce apoptosis. Further experiment is needed to explore the mechanism that induces apoptosis in our model. However, there are a few reports related to the apoptotic pathway induced by Gal-3 depletion. Inhibition of the phosphatidylinositol-3-kinase (PI3K)/Akt signaling pathway was shown to be involved in siGal-3-treated human papillary thyroid cancer cells.[20] Gal-3 also plays role in the Wnt/β-catenin pathway. siRNA silencing of Gal-3 expression inhibited T-cell factor (TCF)-receptor activity, decreased cytosolic β-catenin level, and induced apoptosis in human colorectal cancer cells.[21]

A reduction in the anti-apoptotic activity of Gal-3 in siGal-3-K402-treated cells, however, was readily observable when the cells were exposed to hypoxia or UV-induced apoptotic conditions. Conversely, cells with overexpression of endogenous Gal-3 resisted the above two apoptotic insults. This observation indicated that the GFP-Gal-3 protein produced in Gal-3-overexpressing cells was effectively active.

The correlation of anti-apoptotic activity to the level of Gal-3 expression was also demonstrated in this study. CCA cell line KKU-100, with high endogenous Gal-3, showed higher resistance to apoptotic inductions than did KKU-OCA17 and KKU-M055, which both had lower endogenous Gal-3. These findings suggest the possibility of using expression level of Gal-3 to predict the anti-apoptotic potential of cancer cells or tissues toward chemotherapeutic drugs. This suggestion is supported by the evidence that CCA with high expression of Gal-3 exhibited high chemoresistance whereas those with low expression of Gal-3 were chemosensitive. Among the five human intrahepatic CCA cell lines (KKU-100, KKU-M055, KKU-M156, KKU-M214, and KKU-OCA17), CCA cell line KKU-100, with the highest Gal-3 expression, was highly resistant to all the chemotherapeutic drugs tested, whereas KKU-M055, which does not express Gal-3 constitutively, was the most sensitive.[22] However, this suggestion is a correlative observation and further experimental studies would be needed for a definitive conclusion.

Galectin-3 (Gal-3) seems to be a common key for the anti-apoptotic phenomenon in biological systems. As shown in this study, despite the apoptotic inducers, for example hypoxia and UV irradiation, reduction of Gal-3 expression significantly

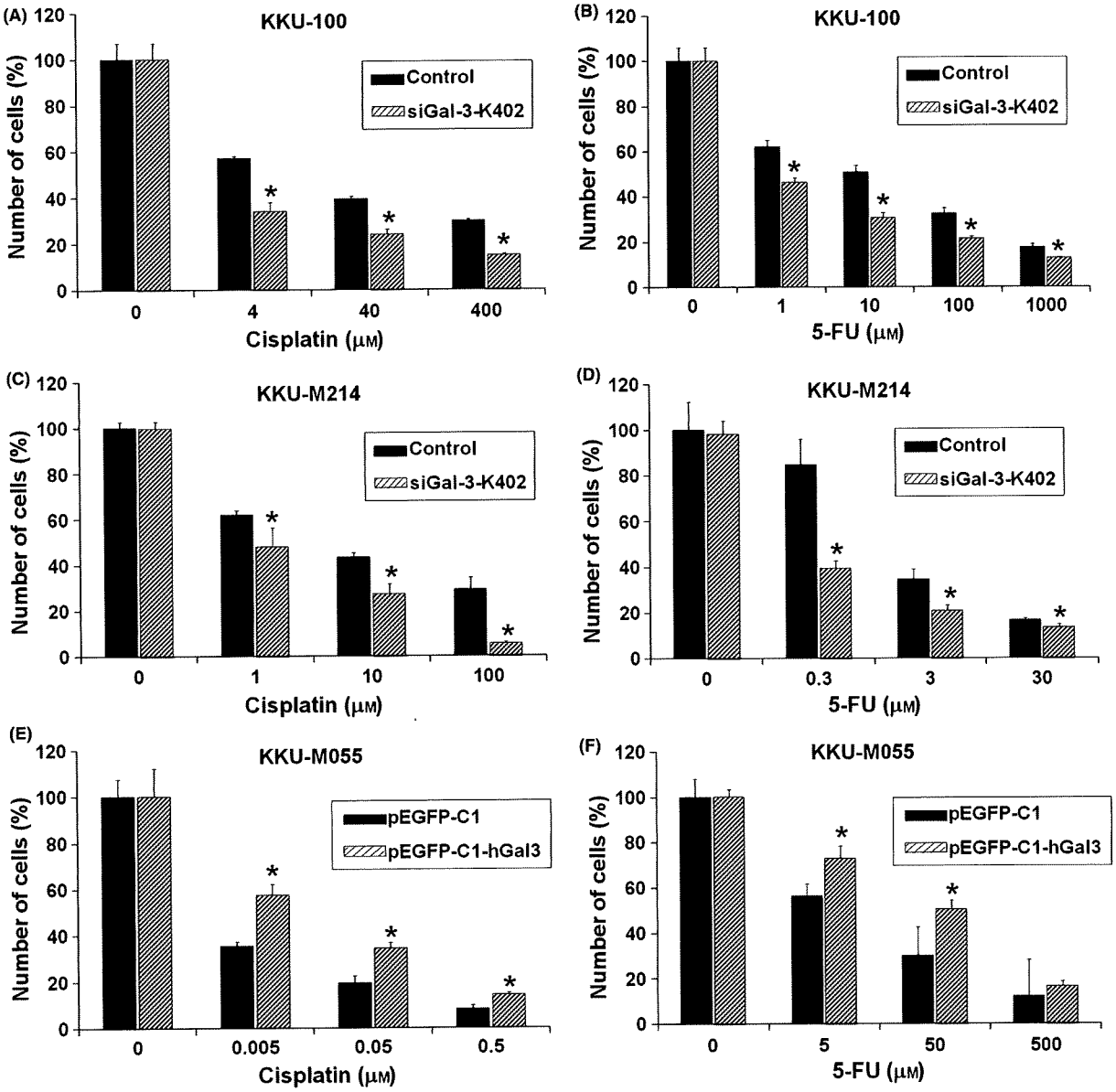

Fig. 5. Galectin-3 (Gal-3) depletion enhances anticancer drug sensitivity whereas overexpressing Gal-3 increases drug resistance. Cholangiocarcinoma (CCA) cell lines KKU-100 or KKU-M214 were treated with either Lipofectamine (black bar) or siGal-3-K402 (slash bar) for 24 h, followed by treatments with various concentrations of cisplatin (A,C) or 5-fluorouracil (5-FU) (B,D) for a further 48 h. KKU-M055 cells were treated with pEGFP-C1 (control, black bar) or pEGFP-C1-hGal3 (Gal-3 overexpressing cells, slash bar) for 24 h, followed by treatments with various concentrations of cisplatin (E) or 5-FU (F) for a further 48 h as above. The number of cells was determined by sulforhodamine-B (SRB) assay. Results are the mean ± SE (bars) of three independent experiments. $^*P < 0.05$.

enhances apoptosis cell death of CCA cells in both conditions. In addition to our study, the anti-apoptotic action of Gal-3 in response to different apoptotic stimulations, anti-Fas-induced cell death and anoikis induced apoptosis, have been reported in B-cell lymphocytes[23] and human breast epithelial cells,[10] respectively.

The finding that Gal-3 plays a role in the anti-apoptosis of CCA cells led to further evaluation as to whether reduction of Gal-3 expression in CCA cells affected their response to the pro-apoptotic action of chemotherapeutic agents. The combined effects of siGal-3 and two chemotherapeutic agents, cisplatin and 5-FU, widely used anticancer agents frequently provided to CCA patients, were evaluated in two CCA cell lines. As expected, the RNAi-mediated knockdown of Gal-3 synergistically enhanced the cytotoxicity of cisplatin and 5-FU in both CCA cell lines. Gal-3 knockdown by RNAi might reduce the anti-apoptotic activity and hence enhance the cytotoxicity of these anticancer drugs. The direct association of Gal-3 suppression with the enhancement of antitumor efficacy was shown in cells overexpressing Gal-3. Increasing Gal-3 expression in KKU-M055 reduced the apoptotic response to anticancer drugs. The nuclear export of phosphorylated galectin-3,[24] translocation of Gal-3 to the perinuclear membrane, and enrichment of Gal-3 in mitochondria[25] have been shown to be the mechanism

doi: 10.1111/j.1349-7006.2009.01304.x

by which galectin-3 regulates its anti-apoptotic activity in response to cisplatin in the BT-549 human breast carcinoma cell line. In the present study, the translocation of Gal-3 from the nucleus to cytoplasm was also observed under apoptotic insult. More experimental data are needed to indicate the definite mechanism by which Gal-3 exerted its anti-apoptotic activity in our study.

Galectin-3 (Gal-3) contains the NWGR (N, asparagine; W, tryptophan; G, glycine; R, arginine) anti-death motif of the Bcl-2 family. One of the mechanisms by which Gal-3 acts on anti-apoptosis in response to anticancer drugs has been shown to be the stimulation of Bcl-2 associated death (Bad) protein phosphorylation and decreasing Bad expression, which resulted in the stabilization of mitochondrial membrane integrity, and subsequently the inhibition of cytochrome *c* release and caspase-3 activation, which finally suppressed apoptosis.[26] Additionally, an anti-apoptotic effect of Gal-3, which is meditated by the activation of the extracellular signal-regulated kinases (ERK) and c-Jun NH_2-terminal kinase (JNK) pathways, is also suggested.[27] The overexpression of Gal-3 probably protects cells from apoptotic death by inhibiting the caspase pathway,[9] or by maintaining mitochondrial homeostasis.[28]

Resistance to chemotherapeutic agents is the major cause of failure for anticancer drug treatment in many cancers, including CCA. Thymidilate synthase, multidrug resistant protein (MRP1), multidrug resistant-associated proteins (MDR3), and glutathione-*S*-transferase 1 (GSTP1) are highly expressed in several CCA cell lines, including KKU-100 and KKU-M214.[22] The actions of these genes may underline the chemo-resistant properties of CCA cells. The finding that the suppression of Gal-3 expression enhances the sensitivity of antitumor drugs suggests the possibility that Gal-3 could be a new target molecule for improving the response of CCA cells to chemotherapeutic drugs.

In conclusion, these results suggest that the expression of Gal-3 provides tumor cells with an anti-apoptotic advantage. Cells with high expression of Gal-3 tend to resist chemotherapeutic treatment, whereas cells with low Gal-3 expression are prone to apoptosis, and hence are sensitive to drug treatment. Based on this observation, Gal-3 expression levels in cancer tissue may be a predictor of chemotherapeutic response, which could help clinicians select an appropriate treatment for CCA patients. Several approaches have been developed to reduce cellular Gal-3 expression. For instance, siGal-3 may be delivered into solid tumors by an efficient delivery system of siRNA[29] that is becoming a conventional application for *in vivo* cancer therapy.[30,31] Synthetic lactulose amines, for example lactulosyl-L-leucine and modified citrus pectin, have been designed and shown to be specific Gal-3 inhibitors for therapeutic purposes.[32] The treatment of cells with modified citrus pectin and lactulosyl-L-leucine was able to abrogate resistance to doxorubicin in angiosarcoma cells.[33] Moreover, the inhibition of Gal-3 anti-apoptotic function by modified citrus pectin was sufficient to reverse multiple myeloma cells' resistance to bortezomib, and enhance their response to apoptosis induced by dexamethasone.[34] Since Gal-3 is frequently expressed in CCA tissues, it is therefore proposed that interfering with Gal-3 action, either by using RNAi-mediated knockdown of Gal-3, or specific Gal-3 inhibitors, can either be developed as a specific gene-targeting therapy to treat CCA, or used in combination with a chemotherapeutic agent to enhance apoptosis and chemosensitivity in CCA.

Acknowledgments

We are grateful for financial support from the Royal Golden Jubilee PhD Program (PHD/0140/2546) to M.J. and S.W.; Grant-in-Aid for Scientific Research on Priority Areas for Cancer Research from The Ministry of Education, Culture, Sports, Science and Technology, Japan (20014021) to Araki N; and the JSPS–Asia Africa Science Platform Program (Khon Kaen University and Kumamoto University). We also thank Professor James Will and Mr. Anthony W. Wilson for assistance with the English-language presentation of the manuscript.

References

1 Vatanasapt V, Tangvoraphonkchai V, Titapant V, Pipitgool V, Viriyapap D, Sriamporn S. A high incidence of liver cancer in Khon Kaen Province, Thailand. *Southeast Asian J Trop Med Public Health* 1990; **21**: 489–94.
2 Haswell-Elkins MR, Mairiang E, Mairiang P *et al.* Cross-sectional study of *Opisthorchis viverrini* infection and cholangiocarcinoma in communities within a high-risk area in northeast Thailand. *Int J Cancer* 1994; **59**: 505–9.
3 Thongprasert S. The role of chemotherapy in cholangiocarcinoma. *Ann Oncol* 2005; **16** (Suppl 2): ii, 93–6.
4 Junking M, Wongkham C, Sripa B, Sawanyawisuth K, Araki N, Wongkham S. Decreased expression of galectin-3 is associated with metastatic potential of liver fluke-associated cholangiocarcinoma. *Eur J Cancer* 2008; **44**: 619–26.
5 Barondes SH, Cooper DN, Gitt MA, Leffler H. Galectins. Structure and function of a large family of animal lectins. *J Biol Chem* 1994; **269**: 20807–10.
6 Hirabayashi J, Kasai K. The family of metazoan metal-independent beta-galactoside-binding lectins: structure, function and molecular evolution. *Glycobiology* 1993; **3** (4): 297–304.
7 Hughes RC. Galectins as modulators of cell adhesion. *Biochimie* 2001; **83**: 667–76.
8 Yang RY, Liu FT. Galectins in cell growth and apoptosis. *Cell Mol Life Sci* 2003; **60**: 267–76.
9 Akahani S, Nangia-Makker P, Inohara H, Kim HR, Raz A. Galectin-3: a novel antiapoptotic molecule with a functional BH1 (NWGR) domain of Bcl-2 family. *Cancer Res* 1997; **57** (23): 5272–6.
10 Kim HR, Lin HM, Biliran H, Raz A. Cell cycle arrest and inhibition of anoikis by galectin-3 in human breast epithelial cells. *Cancer Res* 1999; **59** (16): 4148–54.
11 Lin HM, Moon BK, Yu F, Kim HR. Galectin-3 mediates genistein-induced G(2)/M arrest and inhibits apoptosis. *Carcinogenesis* 2000; **21**: 1941–5.
12 Yang RY, Hsu DK, Liu FT. Expression of galectin-3 modulates T-cell growth and apoptosis. *Proc Natl Acad Sci U S A* 1996; **93** (13): 6737–42.
13 Yoshii T, Fukumori T, Honjo Y, Inohara H, Kim HR, Raz A. Galectin-3 phosphorylation is required for its anti-apoptotic function and cell cycle arrest. *J Biol Chem* 2002; **277** (9): 6852–7.
14 Hsu DK, Yang RY, Pan Z *et al.* Targeted disruption of the galectin-3 gene results in attenuated peritoneal inflammatory responses. *Am J Pathol* 2000; **156** (3): 1073–83.
15 Sripa B, Leungwattanawanit S, Nitta T *et al.* Establishment and characterization of an opisthorchiasis-associated cholangiocarcinoma cell line (KKU-100). *World J Gastroenterol* 2005; **11** (22): 3392–7.
16 Elbashir SM, Harborth J, Weber K, Tuschl T. Analysis of gene function in somatic mammalian cells using small interfering RNAs. *Methods* 2002; **26**: 199–213.
17 Laemmli UK. Cleavage of structural proteins during the assembly of the head of bacteriophage T4. *Nature* 1970; **227** (5259): 680–5.
18 Towbin H, Staehelin T, Gordon J. Electrophoretic transfer of proteins from polyacrylamide gels to nitrocellulose sheets: procedure and some applications. *Proc Natl Acad Sci U S A* 1979; **76** (9): 4350–4.
19 Skehan P, Storeng R, Scudiero D *et al.* New colorimetric cytotoxicity assay for anticancer-drug screening. *J Natl Cancer Inst* 1990; **82** (13): 1107–12.
20 Lin CI, Whang EE, Abramson MA *et al.* Galectin-3 regulates apoptosis and doxorubicin chemoresistance in papillary thyroid cancer cells. *Biochem Biophys Res Commun* 2009; **379**: 626–31.
21 Shi Y, He B, Kuchenbecker KM *et al.* Inhibition of Wnt-2 and galectin-3 synergistically destabilizes beta-catenin and induces apoptosis in human colorectal cancer cells. *Int J Cancer* 2007; **121**: 1175–81.
22 Tepsiri N, Chaturat L, Sripa B *et al.* Drug sensitivity and drug resistance profiles of human intrahepatic cholangiocarcinoma cell lines. *World J Gastroenterol* 2005; **11** (18): 2748–53.
23 Hoyer KK, Pang M, Gui D *et al.* An anti-apoptotic role for galectin-3 in diffuse large B-cell lymphomas. *Am J Pathol* 2004; **164** (3): 893–902.

24 Takenaka Y, Fukumori T, Yoshii T *et al.* Nuclear export of phosphorylated galectin-3 regulates its antiapoptotic activity in response to chemotherapeutic drugs. *Mol Cell Biol* 2004; **24**: 4395–406.
25 Yu F, Finley RL Jr, Raz A, Kim HR. Galectin-3 translocates to the perinuclear membranes and inhibits cytochrome c release from the mitochondria. A role for synexin in galectin-3 translocation. *J Biol Chem* 2002; **277**: 15819–27.
26 Fukumori T, Oka N, Takenaka Y *et al.* Galectin-3 regulates mitochondrial stability and antiapoptotic function in response to anticancer drug in prostate cancer. *Cancer Res* 2006; **66** (6): 3114–9.
27 Fukumori T, Takenaka Y, Yoshii T *et al.* CD29 and CD7 mediate galectin-3-induced type II T-cell apoptosis. *Cancer Res* 2003; **63** (23): 8302–11.
28 Matarrese P, Tinari N, Semeraro ML, Natoli C, Iacobelli S, Malorni W. Galectin-3 overexpression protects from cell damage and death by influencing mitochondrial homeostasis. *FEBS Lett* 2000; **473**: 311–5.
29 Takei Y, Kadomatsu K, Yuzawa Y, Matsuo S, Muramatsu T. A small interfering RNA targeting vascular endothelial growth factor as cancer therapeutics. *Cancer Res* 2004; **64** (10): 3365–70.
30 Hingorani SR, Jacobetz MA, Robertson GP, Herlyn M, Tuveson DA. Suppression of BRAF(V599E) in human melanoma abrogates transformation. *Cancer Res* 2003; **63** (17): 5198–202.
31 Brummelkamp TR, Bernards R, Agami R. Stable suppression of tumorigenicity by virus-mediated RNA interference. *Cancer Cell* 2002; **2**: 243–7.
32 Rabinovich GA, Cumashi A, Bianco GA *et al.* Synthetic lactulose amines: novel class of anticancer agents that induce tumor-cell apoptosis and inhibit galectin-mediated homotypic cell aggregation and endothelial cell morphogenesis. *Glycobiology* 2006; **16** (3): 210–20.
33 Johnson KD, Glinskii OV, Mossine VV *et al.* Galectin-3 as a potential therapeutic target in tumors arising from malignant endothelia. *Neoplasia (New York, NY)* 2007; **9** (8): 662–70.
34 Chauhan D, Li G, Podar K *et al.* A novel carbohydrate-based therapeutic GCS-100 overcomes bortezomib resistance and enhances dexamethasone-induced apoptosis in multiple myeloma cells. *Cancer Res* 2005; **65** (18): 8350–8.

Supporting Information

Additional Supporting Information may be found in the online version of this article:

Fig. S1. Cholangiocarcinoma (CCA) cell line KKU-100 cells were transfected with siGal-3-K626 and the endogenous galectin-3 (Gal-3) was determined by immunoblotting after siRNA transfection for 6, 24, 48, and 72 h. Expression of Gal-3 was gradually suppressed and the effect of siRNA was observed at 6 h before apoptotic induction.

Please note: Wiley-Blackwell are not responsible for the content or functionality of any supporting materials supplied by the authors. Any queries (other than missing material) should be directed to the corresponding author for the article.

doi: 10.1111/j.1349-7006.2009.01304.x

J|A|C|S COMMUNICATIONS

Published on Web 02/25/2009

Silver Ion Unusually Stabilizes the Structure of a Parallel-Motif DNA Triplex

Toshihiro Ihara,*,†,§ Tatsuaki Ishii,† Norie Araki,‡ Anthony W. Wilson,‡ and Akinori Jyo†

Graduate School of Science and Technology, Kumamoto University, 2-39-1 Kurokami, Kumamoto 860-8555, Japan, Graduate School of Medical Sciences, Kumamoto University, 1-1-1 Honjo, Kumamoto 860-8556, Japan, and PRESTO, Japan Science and Technology Agency, San-bancho Building, 3-5 Sanbancho, Chiyodaku, Tokyo 332-0012, Japan

Received December 12, 2008; E-mail: toshi@chem.kumamoto-u.ac.jp

The DNA triple helix is one of the most useful recognition motifs in the design of systems for sequence-specific labeling, regulation of gene expression, and construction of DNA-based nanostructures.[1] It can form in two main ways: an oligopyrimidine strand can bind to the major groove of the duplex parallel to the strand carrying the purine tract using Hoogsteen base-pairing, or alternatively, an oligopurine can bind to the purine strand in an antiparallel orientation using reversed Hoogsteen base-pairing. In the parallel motif, cytosines in the third strand need to be protonated at their N3 positions (pK_a = 4.5) to form CG.C$^+$ base triplets, which stabilize the triplex by favorable electrostatic effects. Therefore, the stability of triplexes containing CG.C$^+$ largely depends on the pH of the solution. While it is more stable than those consisting entirely of TA.T triplets in weakly acidic solution, its stability is very low under physiological conditions.

Several research groups have devoted their efforts to improving the stability of the triplex at neutral pH.[2] These efforts fall into two categories: (1) addition or covalent attachment of auxiliary molecules that alleviate the electrostatic repulsion between the strands or act as a nonspecific anchor[3] and (2) redesign of the DNA backbone and bases.[4] Here we report an effective alternative method for stabilization of the parallel-motif triple helix of DNA using Ag$^+$ ions. To date, several oligodeoxyribonucleotide (ODN) conjugates carrying metal-chelating moieties have been synthesized.[5] Their binding with the targets was regulated by appropriate metal ions through the specific coordination of the appended chelators. Recently, Ono and co-workers[6] reported that the formation of C−C and T−T mispairings in the duplex are promoted by Ag$^+$ and Hg^{2+}, respectively. In the duplexes, the ions were placed between the bases to form specific bridges (C−Ag$^+$−C, T−Hg^{2+}−T). We report the effect of Ag$^+$ on the stability of triplexes containing CG.C$^+$ base triplets. The silver ion is expected to displace an N3 proton of a cytosine in the CG.C$^+$ base triplet to form a CG.CAg$^+$, as shown in Figure 1A. This would stabilize parallel-motif triplexes even at neutral pH.

The sequences of ODNs used in this study are shown in Figure 1B. First, UV melting experiments were carried out for the triplexes **T11/A11/T11** and **TC11/AG11/TC11** at pH 8.5 in the absence and the presence of Ag$^+$.[7] **T11/A11/T11** consists of 11 TA.T triplets. Only the central TA.T triplet was displaced by a CG.C$^+$ in **TC11/AG11/TC11**. The melting curves are shown in Figure 2A. The meltings of the triplexes could be resolved in two steps in the absence of Ag$^+$. The transitions at lower and higher temperatures are attributed to triplex−duplex (t−d) and duplex−coil (d−c) transitions, respectively. Upon addition of Ag$^+$ to **TC11/AG11/TC11**, the t−d transition almost disappeared and merged with the d−c transition. Although this effect was already significant when an equimolar amount of Ag$^+$ for the CG.C$^+$ triplet was added, the shape of the curve around the t−d transition showed a further slight change with additional Ag$^+$. On the other hand, the melting curve of **T11/A11/T11** was scarcely changed by Ag$^+$ titration. Silver ions did not affect the d−c transitions for either

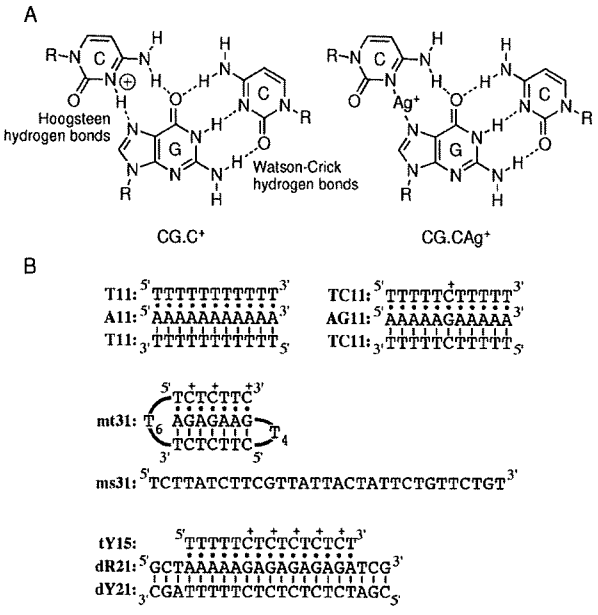

Figure 1. (A) CG.C$^+$ base triplet and the Ag$^+$-mediated base triplet CG.CAg$^+$. (B) Sequences of ODNs used in this study. Bars and dots show Watson−Crick and Hoogsteen base pairings, respectively.

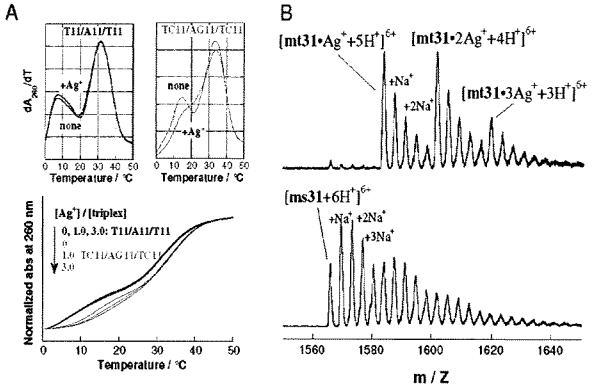

Figure 2. (A) UV melting curves of the triple helixes **T11/A11/T11** (black) and **TC11/AG11/TC11** (red). Each strand (2.5 μM) was dissolved in phosphate buffer (10 mM, pH 8.5) containing 200 mM $NaNO_3$ and 0, 2.5, or 7.5 μM $AgNO_3$. (top) First derivatives of the melting curves obtained in the absence and presence of 7.5 μM Ag$^+$; (bottom) the melting curves. (B) ESI-TOF mass spectra of (top) **mt31** and (bottom) **ms31** in the presence of 1.5 times the amount of Ag$^+$ for possible CG.C$^+$ triplets.

† Graduate School of Science and Technology, Kumamoto University.
‡ Graduate School of Medical Sciences, Kumamoto University.
§ PRESTO.

10.1021/ja809702n CCC: $40.75

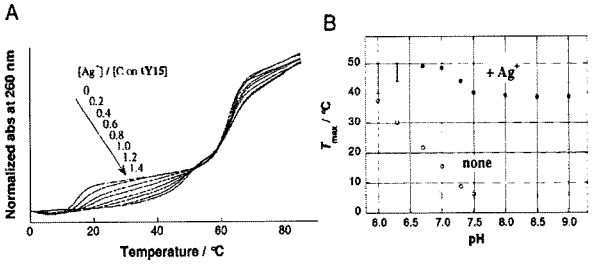

Figure 3. (A) UV melting curves of **dY21/dR21/tY15** obtained in the presence of various amounts of Ag^+. Each strand (2.5 μM) was dissolved in phosphate buffer (10 mM, pH 7.0) containing 200 mM $NaNO_3$ and 0−17.5 μM $AgNO_3$. (B) pH dependence of T_{max} of the t−d transition of **dY21/dR21/tY15** melting in the absence (○) and presence (●) of an equimolar amount of Ag^+ for cytosines in **tY15**.

triplex. Therefore, Ag^+ seems to work only on Hoogsteen hydrogen bonding in the $CG.C^+$ triplet.

To confirm the specific interaction between $CG.C^+$ and Ag^+, **mt31**, which forms an intramolecular triplex structure containing three $CG.C^+$ structures, was subjected to mass spectrometry [(nano)ESI-QqTOF] in the presence of 1.5 times the amount of Ag^+ for the $CG.C^+$ triplet. The spectra are shown in Figure 2B. Almost all of the **mt31** was detected as Ag adducts with a discrete number of Ag^+ (**mt31**·Ag^+, **mt31**·$2Ag^+$, and **mt31**·$3Ag^+$). On the other hand, the control 31-mer ODN **ms31** with a scrambled sequence was mainly detected as several Na adducts of Ag^+-free forms under exactly the same conditions as for **mt31**. The sequence of **ms31** was designed to not form the intramolecular triplex with $CG.C^+$ triplets. These results suggest the specific (but probably not very strong) interaction of Ag^+ with $CG.C^+$ triplets.

The effect of Ag^+ on the stability of the triplex was investigated using the triplex **dY21/dR21/tY15** having multiple $CG.C^+$ triplets in the sequence. UV melting experiments were performed at pH 7.0 in the presence of various amounts of Ag^+ (Figure 3A). Silver ions raised the temperature of the t−d transition, T_{max}, with significant broadening, and eventually, at the equimolar point with cytosine, a new inflection point appeared at 48.7 °C.[8] The stabilization effect of Ag^+ on the binding of the third strand (**tY15**), ΔT_{max}, was more than 30 °C (48.7−16.8 °C). Meanwhile the d−c transition was scarcely affected by Ag^+ addition in this concentration range. This implies that an Ag^+−triplex complex with a certain structure that has its own quite high thermal stability forms at the equimolar point and that in the complex, Ag^+ only affects Hoogsteen base-pairing of $CG.C^+$ triplets. The pH effect on T_{max} was monitored in the absence and the presence of Ag^+. Although T_{max} steadily decreased with rising pH in the absence of Ag^+, the T_{max} values observed in the presence of Ag^+ showed a unique biphasic behavior consisting of two pH-independent regions.[9] The slope of the T_{max}-versus-pH plot is related to the number of protons released when the structures melt to give other forms in equilibrium. As we expected, Ag^+ would displace the N3 proton of cytosine in $CG.C^+$ to form a new triplet, $CG.CAg^+$, below pH 7. Meanwhile, the proton of the exocyclic amino group of cytosine is considered to be dissociated at pH > 7.0 in the presence of Ag^+.[10] Therefore, another pH-independent equilibrium between $CG.C^-Ag^+$ and $CG + C^-Ag^+$ would work in the t−d transition at pH > 8.0. The broadening observed in the transitions before Ag^+ saturation would be derived from the mixture of the triplexes that contain various numbers of Ag^+ on cytosines at different positions, because each of the triplexes should have its own intrinsic thermal stability. Therefore, silver ions are probably incorporated fairly independently into the five binding pockets in **dY21/dR21/tY15** in a saturation process.

To obtain information about the triplex structures, **dY21/dR21/tY15** was subjected to CD measurements [see the Supporting Information (SI)]. While the spectra measured at 7 and 27 °C in the absence of Ag^+ were different, especially in the region of short wavelengths, the corresponding spectra were essentially the same in the presence of Ag^+. This is consistent with the results of the melting experiments shown in Figure 3A. However, the shapes of the CD spectra in the presence of Ag^+ were quite different from the typical spectra of DNA triplexes. The coordination distance in N−Ag^+−N would be longer than that of the Hoogsteen hydrogen bonds in $CG.C^+$. Model studies show that the cytosines on the third strand are forced to be twisted from the plane of Watson−Crick GC pairs in $CG.CAg^+$ triplets (see the SI). This nonplanarity of five $CG.CAg^+$ triplets in **dY21/dR21/tY15** seems to unusually alter the whole structure of the triple helix.

We have shown that Ag^+ remarkably stabilizes the structure of a parallel-motif DNA triplex. Several ligands that specifically bind with DNA triplexes have been developed.[3a,b] The stabilization effect of Ag^+ favorably compares with those for these ligands. This very simple method would be a good choice for the stabilization of DNA triplexes, especially in vitro.

Acknowledgment. This work was partially supported by a Grant-in-Aid for Scientific Research (B) (20350038) from MEXT, Japan. We thank Dr. M. Sugimoto for his advice in the model study.

Supporting Information Available: Additional melting curves and CD spectra of **dY21/dR21/tY15** and the results of DFT calculations for the Ag^+-mediated base triplets. This material is available free of charge via the Internet at http://pubs.acs.org

References

(1) Soyfer, V. N.; Potaman, V. N. *Triple-Helical Nucleic Acids*; Springer: New York, 1995.
(2) Rusling, D. A.; Brown, T.; Fox, K. R. In *Sequence-Specific DNA Binding Agents*; Waring, M., Ed.; RSC Publishing: Cambridge, U.K., 2006; pp 1−22.
(3) (a) Pilch, D. S.; Breslauer, K. J. *Proc. Natl. Acad. Sci. U.S.A.* **1994**, *91*, 9332–9336. (b) Silver, G. C.; Sun, J.-S.; Nguyen, C. H.; Boutorine, A. S.; Bisagni, E.; Hélène, C. *J. Am. Chem. Soc.* **1997**, *119*, 263–268. (c) Li, H.; Broughton-Head, V. J.; Peng, G.; Power, V. E. C.; Ovens, M. J.; Fox, K. R.; Brown, T. *Bioconjugate Chem.* **2006**, *17*, 1561–1567.
(4) (a) Kumar, N.; Nielsen, K. E.; Maiti, S.; Petersen, M. *J. Am. Chem. Soc.* **2006**, *128*, 14–15. (b) Alam, M. R.; Majumdar, A.; Thazhathveetil, A. K.; Liu, J.-L.; Puri, N.; Cuenoud, B.; Sasaki, S.; Miller, P. S.; Seidman, M. M. *Biochemistry* **2007**, *46*, 10222–10233. (c) Rahman, S. M. A.; Seki, S.; Obika, S.; Haitani, S.; Miyashita, K.; Imanishi, T. *Angew. Chem., Int. Ed.* **2007**, *46*, 4306–4309. (d) Shinozuka, K.; Matsumoto, N.; Suzuki, H.; Moriguchi, T.; Sawai, H. *Chem. Commun.* **2002**, 2712–2713.
(5) (a) Tanaka, K.; Tengeiji, A.; Kato, T.; Toyama, N.; Shionoya, M. *Science* **2003**, *299*, 1212–1213. (b) Clever, G. H.; Carell, T. *Angew. Chem., Int. Ed.* **2007**, *46*, 250–253. (c) Kitamura, Y.; Ihara, T.; Tsujimura, Y.; Osawa, Y.; Sasahara, D.; Yamamoto, Y.; Okada, K.; Tazaki, M.; Jyo, A. *J. Inorg. Biochem.* **2008**, *102*, 1921–1931. (d) Ihara, T.; Takeda, Y.; Jyo, A. *J. Am. Chem. Soc.* **2001**, *123*, 1772–1773. (e) Ihara, T.; Sato, Y.; Shimada, H.; Jyo, A. *Nucleosides, Nucleotides Nucleic Acids* **2008**, *27*, 1084–1096.
(6) (a) Miyake, Y.; Togashi, H.; Tashiro, M.; Yamaguchi, H.; Oda, S.; Kudo, M.; Tanaka, Y.; Kondo, Y.; Sawa, R.; Fujimoto, T.; Machinami, T.; Ono, A. *J. Am. Chem. Soc.* **2006**, *128*, 2172–2173. (b) Ono, A.; Cao, S.; Togashi, H.; Tashiro, M.; Fujimoto, T.; Machinami, T.; Oda, S.; Miyake, Y.; Okamoto, I.; Tanaka, Y. *Chem. Commun.* **2008**, 4825–4827.
(7) We first attempted the melting experiments at pH 7. However, the triplex **TC11/AG11/TC11** melted almost cooperatively. To evaluate both transitions (t−d and d−c) separately, the pH was raised to 8.5.
(8) The maximum temperatures of the first derivative of the melting curves, T_{max}, were used as the indicators of triplex stabilities.
(9) T_{max} values around pH 6 were not precisely determined because the t−d transitions became broad, as in the melting curves before Ag^+ saturation measured at pH 7 (Figure 3A). However, the curves became sharper upon further addition of Ag^+ (2 times for C). This supports the idea of proton displacement by Ag^+ in the $CG.C^+$ base triplet.
(10) (a) Daune, M.; Dekker, C. A.; Schachman, H. K. *Biopolymers* **1966**, *4*, 51–76. (b) Eichhorn, G. L.; Butzow, J. J.; Clark, P. *Biopolymers* **1966**, *5*, 283–296.

JA809702N

European Journal of Pharmaceutical Sciences 38 (2009) 249–261

Contents lists available at ScienceDirect

European Journal of Pharmaceutical Sciences

journal homepage: www.elsevier.com/locate/ejps

Involvement of PI3K-Akt-Bad pathway in apoptosis induced by 2,6-di-O-methyl-β-cyclodextrin, not 2,6-di-O-methyl-α-cyclodextrin, through cholesterol depletion from lipid rafts on plasma membranes in cells

Keiichi Motoyama[a], Kazuhisa Kameyama[a], Risako Onodera[a], Norie Araki[b], Fumitoshi Hirayama[c], Kaneto Uekama[c], Hidetoshi Arima[a,*]

[a] Graduate School of Pharmaceutical Sciences, Kumamoto University, 5-1 Oe-honmachi, Kumamoto 862-0973, Japan
[b] Graduate School of Medical Sciences, Kumamoto University, Kumamoto 860-8556, Japan
[c] Faculty of Pharmaceutical Sciences, Sojo University, Kumamoto 860-0082, Japan

ARTICLE INFO

Article history:
Received 9 May 2009
Received in revised form 19 July 2009
Accepted 26 July 2009
Available online 5 August 2009

Keywords:
Apoptosis
2,6-Di-O-methyl-β-cyclodextrin
2,6-Di-O-methyl-α-cyclodextrin
Cholesterol
Lipid rafts
PI3K-Akt-Bad

ABSTRACT

Cyclodextrins (CyDs), which are widely used to increase the solubility of drug in pharmaceutical fields, are known to induce hemolysis and cytotoxicity at high concentrations. However, it is still not unclear whether cell death induced by CyDs is apoptosis or not. Therefore, in the present study, we investigated the effects of various kinds of CyDs on apoptosis in the cells such as NR8383 cells, A549 cells and Jurkat cells. Of various CyDs, methylated CyDs inducted cell death under the present experimental conditions, but hydroxypropylated CyDs or sulfobutyl ether-β-CyD (SBE7-β-CyD) did not. Of methylated CyDs, 2,6-di-O-methyl-β-cyclodextrin (DM-β-CyD) and 2,3,6-tri-O-methyl-β-cyclodextrin (TM-β-CyD) markedly caused apoptosis in NR8383 cells, A549 cells and Jurkat cells, through cholesterol depletion in cell membranes. In sharp contrast, 2,6-di-O-methyl-α-cyclodextrin (DM-α-CyD) and methyl-β-cyclodextrin (M-β-CyD) induced cell death in an anti-apoptotic mechanism. DM-β-CyD induced apoptosis through the inhibition of the activation of PI3K-Akt-Bad pathway. Neither p38 MAP kinase nor p53 was contributed to the induction of apoptosis by DM-β-CyD. Additionally, DM-β-CyD significantly decreased mitochondrial transmembrane potential, and then caused the release of cytochrome c from mitochondria to cytosol in NR8383 cells. Furthermore, we confirmed that down-regulation of pro-caspase-3 and activation of caspase-3 after incubation with DM-β-CyD. These results suggest that of methylated CyDs, DM-β-CyD, not DM-α-CyD, induces apoptosis through the PI3K-Akt-Bad pathway, resulting from cholesterol depletion in lipid rafts of cell membranes.

1. Introduction

There are three forms of cell death: apoptosis, autophagic cell death, and necrosis (Edinger and Thompson, 2004). Recently, the additional form of cell death, a programmed necrosis, has been reported (Zong et al., 2004; Tu et al., 2009). Among the four distinct forms of cell death, apoptosis is best studied. Apoptosis is roughly defined by morphological and biochemical changes of the cells (Allen et al., 1997; Taatjes et al., 2008; Loos and Engelbrecht, 2009). Two distinct apoptotic signaling pathways, i.e. mitochondrial-dependent and -independent pathways control apoptosis activation. Intracellular cues, such as damage to the cell's DNA, drive apoptosis primarily through the mitochondrial-dependent pathway, while extracellular signals, usually generated by cytotoxic cells of immune system, trigger apoptosis mainly through the mitochondrial-independent pathway (Ashkenazi, 2008). Both pathways stimulate pro-apoptotic caspase, a family of cysteine proteases, as pro-caspases and are activated through a process called 'the caspase cascade' (Kim et al., 2005; Lavrik et al., 2005).

Membrane lipids are known to be associated with cell death. Cholesterol is an abundant component of the plasma membrane of eukaryotic cells, which plays a pivotal role in the regulation of membrane fluidity, permeability, receptor function and ion channel activity (Brown and London, 1998; Burger et al., 2000; Simons and Toomre, 2000; Edidin, 2003). The lateral distribution of cholesterol in the membrane is not uniform and its content is particularly high in lipid rafts (Dobrowsky, 2000). These microdomains have been reported to act as molecular platforms that spatially organize membrane receptor molecules such as epidermal growth factor

* Corresponding author. Tel.: +81 96 371 4160; fax: +81 96 371 4420.
E-mail address: arimah@gpo.kumamoto-u.ac.jp (H. Arima).

0928-0987/$ – see front matter © 2009 Elsevier B.V. All rights reserved.
doi:10.1016/j.ejps.2009.07.010

(EGF) receptor and CD95 (Fas) (Simons and Toomre, 2000; Dykstra et al., 2003; Bollinger et al., 2005). This reorganization is of crucial importance in the initiation and regulation of inflammatory processes and apoptosis. For example, redistribution of death receptors such as Fas to cholesterol-enriched lipid domains has been proposed to be an important regulatory step during the activation of the apoptotic death program (Grassme et al., 2001; Lacour et al., 2004). Meanwhile, phosphoinositides such as phosphatidylinositol 3,4,5-trisphosphate and phosphatidylinositol 3,4-bisphosphate promote cell survival and protect against apoptosis by activating Akt/PKB, which phosphorylates components of the apoptotic machinery (Mejillano et al., 2001). In addition, ceramides which serve as intermediates for sphingolipids, a major component of cell membranes have been implicated as signaling molecules, and in response to various stresses such as hypoxia and restricted blood supply (ischemia), total cellular ceramide concentration increases, which in turn can activate molecules that induce apoptosis (Crowder, 2009). Therefore, the regulation of membrane lipids levels in lipid rafts is one of the key factors of apoptotic signal in cells.

Cyclodextrins (CyDs) and their hydrophilic derivatives form inclusion complexes with hydrophobic molecules. CyDs can improve the solubility, dissolution rate and bioavailability of the drugs, and so the widespread use of CyDs is well known in the pharmaceutical field (Uekama et al., 1998; Szente and Szejtli, 1999). CyDs have been reported to interact with cell membrane constituents such as cholesterol and phospholipids, resulting in the induction of hemolysis of human and rabbit red blood cells (RRBC) (Irie et al., 1982; Ohtani et al., 1989; Fauvelle et al., 1997). Additionally, we have reported that CyDs-induced hemolysis at high concentration: the magnitude of hemolytic activity of CyDs in human erythrocytes increased in the order of γ-CyD < α-CyD < 2-hydroxypropyl-β-CyD (HP-β-CyD) < β-CyD < 2,3,6-tri-*O*-methyl-β-CyD (TM-β-CyD) < 2,6-di-*O*-methyl-β-CyD (DM-β-CyD) and there is a positive correlation between the hemolytic activity of CyDs and their capacity to solubilize cholesterol (Irie and Uekama, 1997).

Numerous studies regarding the disruption of lipid rafts by CyDs have been reported (Kabouridis et al., 2000; Parpal et al., 2001). It is well known that methyl-β-CyD (M-β-CyD) disrupts lipid rafts through extraction of cholesterol from cell membranes and alters cell signaling at the cell surface in cell biology (Gniadecki, 2004; Hueber et al., 2002). Recently, we reported that DM-β-CyD and M-β-CyD induced morphological change of RRBC from discocyte to echinocyte through the extraction of cholesterol from cholesterol-rich lipid rafts (Motoyama et al., 2009), while 2,6-di-*O*-methyl-α-CyD (DM-α-CyD) induced morphological changes from discocyte to stomatocyte by the extraction of sphingomyelin from sphingolipid-rich lipid rafts, but not extraction of cholesterol (Motoyama et al., 2009). These lines of evidence make it tempting to speculate that DM-β-CyD and DM-α-CyD show the differential type of cell death, because these CyDs extract membrane constituents from the different lipid microdomains on RRBC membranes. However, it is still not unclear whether these CyDs induce apoptosis or not through the interaction with membrane components in various kinds of cells. Therefore, in the present study, we examined whether cell death induced by CyDs is apoptosis or not toward various cells such as NR8383 cells; rat alveolar macrophage cell line, A549 cells; human lung adenocarcinoma epithelial cell line, and Jurkat cells; human T cell lymphoblast-like cell line. To gain insight into the mechanism for this apoptotic effect of DM-β-CyD, the involvement of apoptotic signaling pathways of PI3K-Akt, MAP kinase, p53, cytochrome c and caspase-3 in apoptosis induced by DM-β-CyD was studied. Finally, we discussed the effects of the type of lipid rafts on apoptosis and the potential use of DM-β-CyD as well as TM-β-CyD as novel antitumor agents.

Table 1
Chemical structures of CyD derivatives used in this study.

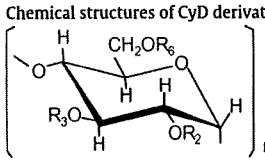

Compound	*n*	R2, R3, R6	DS[a]
α-CyD	6	H	–
β-CyD	7	H	–
γ-CyD	8	H	–
M-β-CyD[b]	7	H or CH_3	12.6
DM-α-CyD[c]	6	R_2, R_6=CH_3, R_3=H	12
DM-β-CyD[d]	7	R_2, R_6=CH_3, R_3=H	14
TM-β-CyD[e]	7	R_2, R_3, R_6=CH_3	21
HP-α-CyD[f]	6	H or CH_2 $CH(OH)CH_3$	4.1
HP-β-CyD[g]	7	H or $CH_2CH(OH)CH_3$	4.8
SBE7-β-CyD[h]	7	H or $(CH_2)_4SO_3Na$	6.2

[a] Average degree of substitution.
[b] Methyl-β-CyD.
[c] 2,6-Di-*O*-methyl-α-CyD.
[d] 2,6 -Di-*O*-methyl-β-CyD.
[e] 2,3,6-Tri-*O*-methyl-β-CyD.
[f] 2-Hydroxypropyl-α-CyD.
[g] 2-Hydroxypropyl-β-CyD.
[h] Sulfobutyl ether-β-CyD.

2. Materials and methods

2.1. Materials

CyDs used in the present study are depicted in Table 1. α-, β-, γ-CyD, 2-hydroxypropyl-α-CyD (HP-α-CyD), HP-β-CyD, 2-hydroxypropyl-γ-CyD (HP-γ-CyD) and DM-β-CyD were gifted from Nihon Shokuhin Kako (Tokyo, Japan). M-β-CyD (average degree of substitution = 10.5–14.7 per 7 glucose unit) was purchased from Sigma (St. Louis, MO). DM-α-CyD and TM-β-CyD were purchased from Wako Pure Chemical Industries (Osaka, Japan). Sulfobutyl ether β-CyD (SBE7-β-CyD) was gifted from CyDex (Lenexa, KS). F-12K culture medium, rhodamine 123 and propidium iodide (PI) were purchased from Invitrogen (Carlsbad, CA). Fetal calf serum (FCS) was obtained from JRH Biosciences (Renexa, KS). Hoechst 33342 and glutaraldehyde were obtained from Sigma (St. Louis, MO) and Nacalai Tesque (Kyoto, Japan), respectively. All other chemicals and solvents were of analytical reagent grade.

2.2. Preparation of macrophages

C57BL/6 mice (8–9 weeks old, wild type and $p53^{-/-}$) were injected with 1.0 ml of 3% thioglycollate intraperitoneally. On day 4, the peritoneal exude cells (PEC) were obtained by peritoneal lavage with 10 ml of ice-cold Hanks' balanced salt solution (HBSS, Ca^{2+} and Mg^{2+} free) supplemented with 10 U/ml of heparin. PEC were washed twice and resuspended in RPMI-1640 medium supplemented with 10% FCS, and overlaid on plastic culture plates. The plates were incubated in humidified 5% CO_2 for 2 h at 37 °C to allow macrophage adherence. Each plate was washed with gentle agitation by warmed RPMI-1640 to dislodge non-adherent cells, and a macrophage monolayer was obtained.

2.3. Cell viability

Cell viability was assayed by the WST-1 method (a Cell Counting Kit, Wako Pure Chemical Industries, Osaka, Japan), as reported previously (Hamasaki et al., 1996; Ono et al., 2001). Briefly, NR8383 cells, A549 cells and Jurkat cells were seeded at 5×10^4 cells onto

96-well microplate (Iwaki, Tokyo, Japan) and incubated for 2 h in a humidified atmosphere of 5% CO_2 and 95% air at 37 °C. Cells were washed twice with phosphate-buffered saline (PBS, pH 6.5), and then incubated for 1 h with 150 μL of F-12K culture medium supplemented with 15% FCS containing CyDs or Tween 20 at various concentrations in a humidified atmosphere of 5% CO_2 and 95% air at 37 °C. After washing twice with PBS to remove CyDs, 100 μL of fresh HBSS (pH 7.4) and 10 μL of WST-1 reagent were added to the plates and incubated for 1 h at 37 °C. The absorbance at 450 nm against a reference wavelength of 630 nm was measured with a miniplate reader (Nalge Nunc International NJ-2300, Rochester, NY).

2.4. Flow cytometry analysis

For determination of DNA content in cells, NR8383 cells (4×10^5) on 24-well culture plate (Iwaki, Tokyo, Japan) were incubated with culture medium containing CyDs for 24 h. After washing with PBS, cells were suspended and fixed with 100 μL of ice-cold 70% (v/v) ethanol for 3 h. After washing with PBS and subsequent centrifugation, cells were re-suspended with RNase A (100 μg/ml) and incubated for 30 min at 37 °C. After centrifugation, cells were re-suspended in a solution containing 100 μL of PI (20 μg/ml) and incubated for 20 min on ice before quantification using a FACSCalibur flow cytometer with CellQuest software (Becton Dickinson, Mountain View, CA).

Translocation of phosphatidylserine (PS) was detected by Tacs™ AnnexinV-FITC Apoptosis Detection Kits (R&D Systems, MN). NR8383 cells (1×10^5) and murine peritoneal macrophages obtained from wild type and $p53^{-/-}$ C57BL/6 mice (1×10^5) on 35-mm dish (Iwaki, Tokyo, Japan) were incubated with 5 mM CyDs containing culture medium for 24 h. After washed by PBS, the cells were stained with annexinV-FITC and PI followed by flow cytometry analysis as described above.

To measure the mitochondrial transmembrane potential ($\Delta\psi_m$), rhodamine 123 was used as reported previously (Emaus et al., 1986). NR8383 cells (1×10^6) on 60-mm dish (Iwaki, Tokyo, Japan) were incubated with culture medium containing 5 mM CyDs for 24 h. After washed with PBS, cells were stained by rhodamine 123 (10 μM) for 15 min at 37 °C. Then, $\Delta\psi_m$ was analyzed by a FACSCalibur flow cytometer as described above.

2.5. DNA fragmentation assay

NR8383 cells (1×10^5/35-mm dish) were incubated with culture medium containing 5 mM CyDs for 24 h. After washed with PBS, lysis buffer (10 mM Tris–HCl (pH 8.0), 10 mM EDTA·4Na, 0.5% Triton X-100) was added to the cells, and then incubated with RNase A (400 μg/ml) for 30 min at 37 °C. Furthermore, the cells were incubated with proteinase K (final concentration: 400 μg/ml) for 1 h at 50 °C. Gel electrophoresis was carried out at room temperature in TBE buffer (45 mM Tris–borate, 1 mM EDTA, pH8.0) in 2% agarose gel containing ethidium bromide (0.1 μg/ml) using Mupid™ system (Cosmo Bio, Tokyo, Japan) at 100 V for 40 min. The fragment DNA bands were visualized using an UV illuminator.

2.6. Determination of chromatin condensation

NR8383 cells were cultured in a glass-based 30 mm dish. After washed twice with PBS, the cells were incubated with 5 mM CyDs in culture medium for 24 h at 37 °C. After washed with PBS, the cells were fixed with 4% glutaraldehyde for 40 min. After incubation with 10 μg/ml of Hoechst 33342 in PBS for 10 min at 37 °C, the cells were scanned using the confocal fluorescence microscopic system (Olympus FV300-BX, Tokyo, Japan).

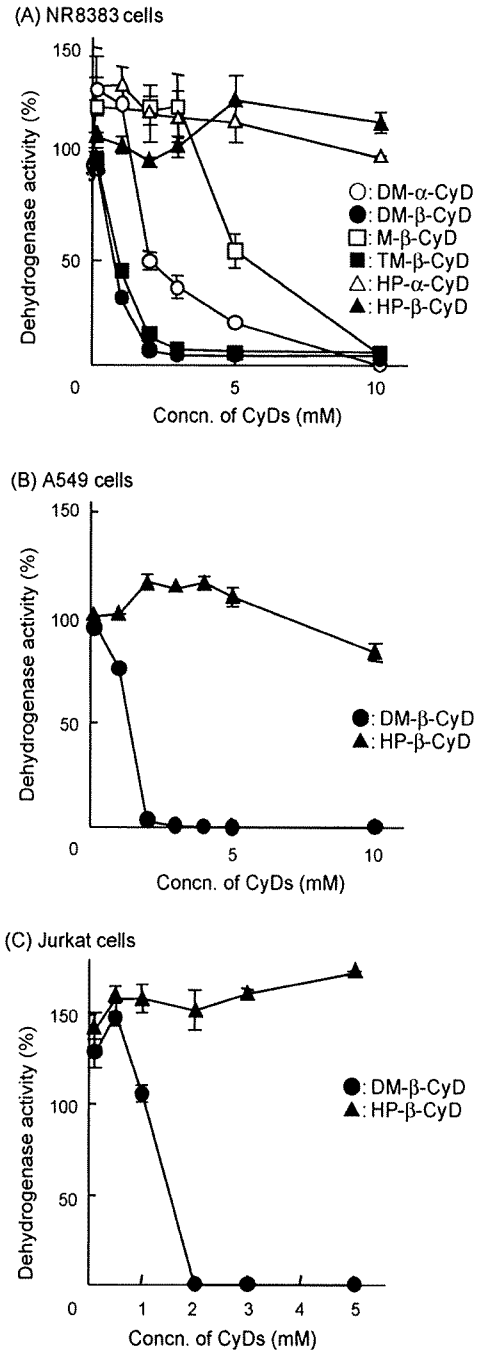

Fig. 1. Cytotoxicity of CyDs in NR8383 cells (A), A549 cells (B) and Jurkat cells (C). Cells were incubated with medium containing CyDs (0–10 mM) at 37 °C for 24 h. After washing twice with HBSS, cell viability was assayed by the WST-1 method. Each point represents the mean ± S.E.M. of three experiments.

2.7. Determination of phospholipids and cholesterol in supernatant

After NR8383 cells (1×10^5/35-mm dish) were incubated with CyDs in HBSS at 37 °C for 1 h, the cell suspension was centrifuged at 10,000 rpm for 10 min. Total phospholipids in supernatant were determined using a Phospholipids-test Wako® (Wako Pure Chemical Industries, Osaka, Japan). For the cholesterol determination, the resulting supernatant (0.5 ml) was mixed with 1 ml of chloroform/methanol (15:2, v/v). After shaking for 10 min, the

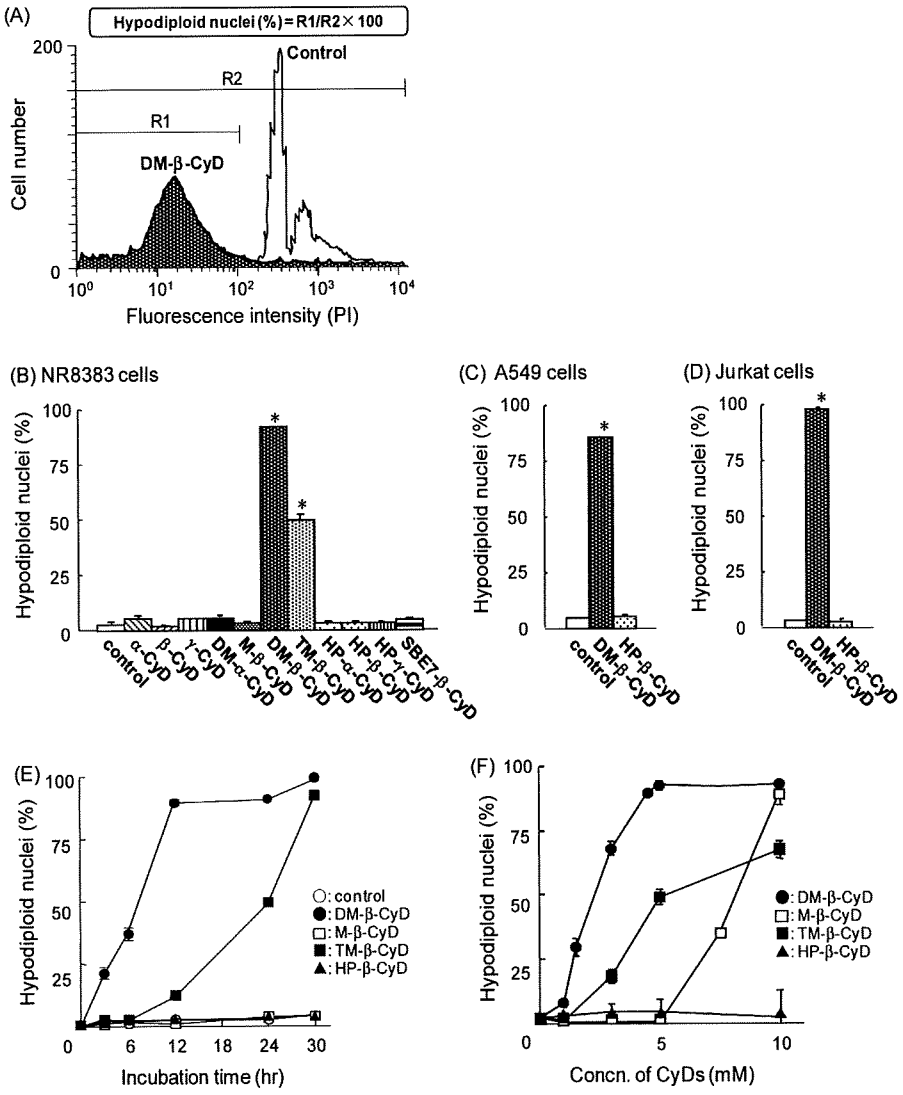

Fig. 2. Flow cytometric analysis of DNA content in NR8383 cells (A and B), A549 cells (C) and Jurkat cells (D) after treatment with 5 mM CyDs. Effects of incubation time of CyDs (E) and CyD-concentration (F) on DNA content in NR8383 cells. After incubation with CyDs for 24 h at 37 °C, the cells were stained by PI, and the percentage of cells showing DNA degradation was quantified by flow cytometry. Each value represents the mean ± S.E.M. of three experiments. *$p < 0.05$ *versus* control.

phase of chloroform was recovered and evaporated to concentrate membrane components. The concentrations of cholesterol in supernatants were determined using a Cholesterol-test Wako® (Wako Pure Chemical Industries, Osaka, Japan).

2.8. Western blot analysis

Akt, phospho-Akt, Bad, phospho-Bad, cytochrome *c*, and cytochrome oxidase IV in NR8383 cells were detected by Western blot analysis as reported previously (Li et al., 2006). Briefly, NR8383 cells (5×10^6 cells/60-mm dish) were incubated with 5 mM CyDs for 24 h. After washing with PBS, cells were lysed with 4× sample buffer (8% SDS, 40% glycerol, 24% β-mercaptoethanol in Tris–HCl buffer (pH 6.8)) and boiled for 5 min. After determining protein concentrations using the bicinchoninic acid reagent from Pierce Chemical (Rockford, IL), samples (20 μg as proteins) were separated with 10% (for the assay of Akt, phosphor-Akt and actin) and 15% (for the assay of Bad, phosphor-Bad, cytochrome *c* and cytochrome oxidase IV) SDS-PAGE and transferred onto Immobilon P membranes (Nihon Millipore, Tokyo, Japan). The membranes were blocked with 5% skim milk in PBS containing 0.1% Tween 20 (PBS-T) and incubated with primary antibody (rabbit anti-Akt antibody), mouse anti-phospho-Akt antibody (Cell Signaling, Beverly, MA), mouse anti-Bad antibody, rabbit anti-phospho-Bad antibody, rabbit anti-actin antibody, rabbit anti-caspase-3 antibody (Santa Cruz, DE, CA), mouse anti-cytochrome *c* antibody and mouse anti-cytochrome oxidase subunit IV antibody (BD Pharmingen, Franklin, NJ) at 4 °C for overnight. After washing with PBS-T, the membranes were incubated with secondary antibody of peroxidase-conjugated sheep anti-mouse IgG antibody or peroxidase-conjugated donkey anti-rabbit IgG antibody (Amersham-pharmacia Biotech, Buckinghamshire, UK). Specific bands were detected using an ECL Western blotting analysis kit (Amersham Bioscience, Tokyo, Japan). The bands were detected using the Lumino-image analyzer LAS-1000 plus (Fujifilm, Tokyo, Japan).

2.9. Statistical analysis

Data are given as the mean ± S.E.M. Statistical significance of means for the studies was determined by analysis of variance

followed by Scheffe's test. p-Values for significance were set at 0.05.

3. Results

3.1. DM-β-CyD and TM-β-CyD induced apoptosis in NR8383 cells

The extent of cytotoxic activity of CyDs depends on the concentration of CyDs and the type of cells. Firstly, we examined cell viability in various cells after incubation with CyDs using by the WST-1 method. HP-α-CyD or HP-β-CyD did not decrease cell viability to NR8383 cells up to 10 mM after 24 h incubation (Fig. 1A). On the other hand, methylated CyD derivatives markedly reduced the viability of the cells in the order of M-β-CyD < DM-α-CyD < TM-β-CyD < DM-β-CyD. In addition, the strong cytotoxic activity of DM-β-CyD, not HP-β-CyD, in A549 cells and Jurkat cells was also observed (Fig. 1B and C). Thus, methylated CyDs strongly interact with various cells, compared to HP-CyDs.

To investigate whether methylated CyDs-induced cell death is accompanied by apoptotic feature, we next examined both the DNA content in nucleus and chromosomal DNA fragmentation using a flow cytometry and an agarose gel electrophoresis, respectively. Actually, the DNA content in nucleus was detected by the addition of PI through the intercalation into double strand DNA calculated as hypodiploid nuclei (%). The DNA content in nucleus after incubation with 5 mM DM-β-CyD for 24 h was strikingly decreased, compared to that in control (without CyD) in NR8383 cells (Fig. 2A). Fig. 2B shows the effects of CyDs on the DNA content in nucleus after incubation with various CyDs (5 mM) for 24 h in NR8383 cells. Of methylated CyDs, DM-β-CyD and TM-β-CyD, not DM-α-CyD or M-β-CyD, strikingly lowered the DNA content in the nucleus of the cells under the experimental conditions where complete cell death occurred (Figs. 1A and 2B). The DNA contents in nucleus in both A549 cells and Jurkat cells were also decreased by the treatment with DM-β-CyD (Fig. 2C and D). The decreasing DNA content by the treatment with DM-β-CyD or TM-β-CyD was incubation time-dependent and concentration-dependent (Fig. 2E and F). Meanwhile, no significant decrease in the DNA content was observed in natural CyDs, M-β-CyD, hydroxypropylated CyDs or SBE7-β-CyD in NR8383 cells (Fig. 2B), suggesting the safety profiles of these CyDs, consistent with previous findings of these CyDs (Irie and Uekama, 1997; Rajewski et al., 1995). Interestingly, DM-α-CyD did not change the DNA content even under the experimental condition where 80% of cell death was inducted (Fig. 2B). As shown in Fig. 3, the agarose gel electrophoresis study revealed that DNA fragmentation in NR8383 cells occurred after incubation with DM-β-CyD or TM-β-CyD. Additionally, DNA fragmentation caused by DM-β-CyD was incubation time-dependent and concentration-dependent (Fig. 3B and C).

Next, we observed the morphological changes in NR8383 cells after incubation with β-CyDs for 24 h using a fluorescence microscopy. To visualize the chromatin condensation in cells, Hoechst 33342 was used as a DNA-binding fluorescence dye. Condensed and segmented nuclei were observed in the cells treated with DM-β-CyD and TM-β-CyD, but neither M-β-CyD nor HP-β-CyD (Fig. 4). These results are well consistent with the results of DNA content analysis and DNA fragmentation analysis (Figs. 2 and 3). These findings suggest that DM-β-CyD and TM-β-CyD induce apoptosis in NR8383 cells.

3.2. Effects of methylated CyDs on PS externalization

A critical event during apoptosis appears to be the acquisition of plasma membrane changes that allows phagocytes to recognize and engulf these cells before they rupture. Then, we next examined the effects of methylated CyDs on PS externalization in early apoptotic cells. The treatment of NR8383 cells with 5 mM DM-β-CyD or TM-β-CyD for 24 h significantly increased in the number of annexinV-FITC(+)/PI(−) cells as early apoptosis (Fig. 5A and B), however, the treatment with 5 mM DM-α-CyD, HP-β-CyD or M-β-CyD did not increase them, although cell death occurred under the present experimental conditions (Fig. 1A). In addition, we confirmed that the extent of PS externalization after treatment with DM-β-CyD increased in a time-dependent manner (data not shown). These results strongly suggest that cell death induced by DM-β-CyD and TM-β-CyD results from apoptosis.

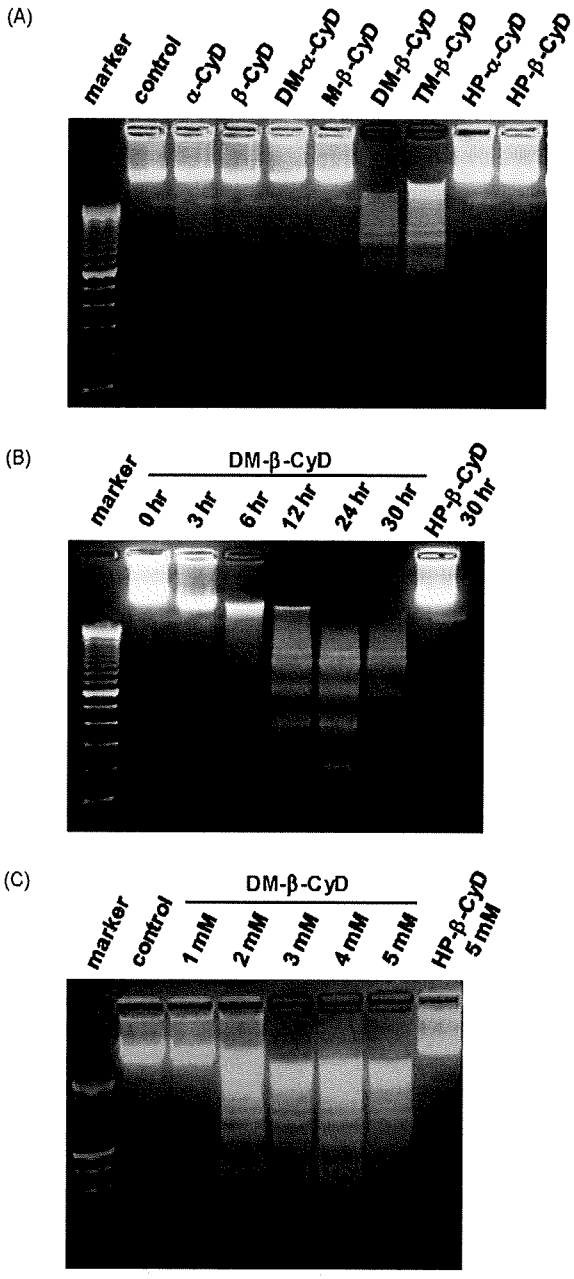

Fig. 3. (A) Agarose gel electrophoresis of DNA extracted from NR8383 cells treated with CyDs. Time-dependent effect (B) and concentration-dependent effect (C) of CyDs on apoptosis in NR8383 cells were shown. NR8383 cells were incubated with medium containing CyDs at 1 mM for 24 h at 37 °C. After incubation, cells were lysed and then analyzed DNA fragmentation using a gel electrophoresis.

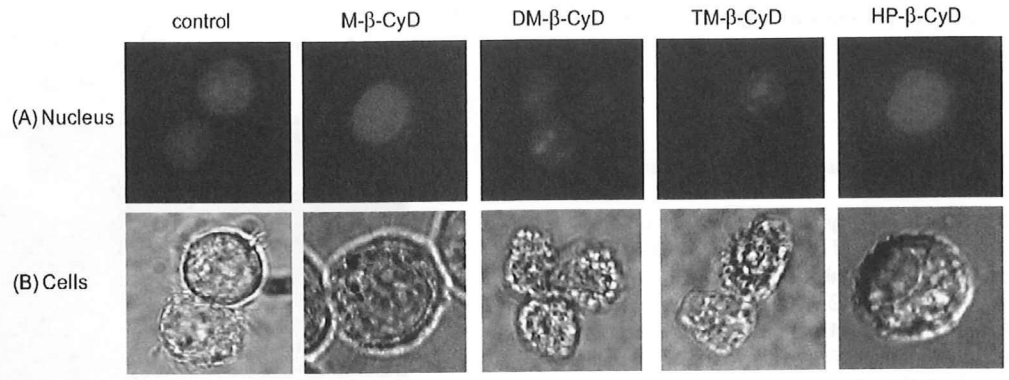

Fig. 4. Fluorescence (A) and phase contrast (B) micrographs of NR8383 cells treated with β-CyDs. After incubation with medium containing β-CyDs (5 mM) for 24 h at 37 °C, NR8383 cells were stained by Hoechst 33342, and condensations of chromatin were detected using a fluorescence microscope.

3.3. Membrane lipids such as cholesterol and phospholipids released by CyDs

Lipid rafts are mainly composed of cholesterol and sphingolipids such as sphingomyelin in the cell membranes, and contain various signal transduction molecules including growth factor receptors (Le Roy and Wrana, 2005). We previously reported that CyDs showed hemolytic activity at high concentrations through the extraction of cell membrane components such as cholesterol and phospholipids in cell membranes (Ohtani et al., 1989; Irie and Uekama, 1997). Recently, we reported that DM-β-CyD induced morphological change of RRBC to echinocyte through the extraction of cholesterol from cholesterol-rich lipid rafts (Motoyama et al., 2009), while DM-α-CyD induced morphological changes to stomatocyte by the extraction of sphingomyelin from sphingolipid-rich lipid rafts, but not extraction of cholesterol (Motoyama et al., 2009). Therefore, to gain insight into the mechanism of apoptosis induced by DM-β-CyD and TM-β-CyD, we investigated that the effects of CyDs on the release of cholesterol and phospholipids from NR8383 cells. Cholesterol and phospholipids released in supernatant after incubation with 5 mM CyDs for 1 h were determined by Cholesterol-test Wako® and Phospholipids-test Wako®, respectively. The extent of cholesterol released from NR8383 cells by treated with β-CyDs was increased in the order of DM-α-CyD ≪ HP-β-CyD < M-β-CyD < TM-β-CyD < DM-β-CyD (Fig. 6A). Meanwhile, DM-α-CyD and DM-β-CyD remarkably released phospholipids in the supernatant, but the others did not (Fig. 6B). These results suggest that DM-β-CyD and TM-β-CyD induced apoptosis through the cholesterol depletion in cell membranes. Next, we examined whether apoptosis induced by the treatment with DM-β-CyD is suppressed by the addition of cholesterol in culture medium using a flow cytometry. As shown in Fig. 6C, apoptosis induced by DM-β-CyD in NR8383 cells was significantly suppressed by the addition of cholesterol. These results suggest that DM-β-CyD induces apoptosis through cholesterol depletion from cell membranes.

3.4. DM-β-CyD induced apoptosis in NR8383 cells via PI3K-Akt-Bad pathway

It is well known that Akt kinase activity is induced following PI3K activation in various growth factor receptor-mediated signaling cascades (Franke et al., 2003). On the other hand, p38 MAPK is stress-activated protein kinase and has an important role in apoptotic signal transduction (Davis, 2000). Therefore, we next investigated the effects of DM-β-CyD on PI3K-Akt and MAPK pathways. Hereafter, we employed HP-β-CyD as a negative control because of the lack of apoptotic activity under the experimental conditions. Apoptosis induced by DM-β-CyD was significantly increased by the pretreatment of NR8383 cells with LY294002, a PI3K specific inhibitor (Fig. 7A). However, no significant change was observed in pretreatment with SB203580, a p38 MAP kinase inhibitor in NR8383 cells (Fig. 7B). These results suggest that apoptosis induced by DM-β-CyD is involved in PI3K rather than p38 MAP kinase. Next, we investigated the effects of DM-β-CyD on Akt activation. Then, Akt and its activating form (phospho-Akt) were determined by Western blot analysis using an anti-Akt antibody and anti-phospho-Akt antibody, respectively. As shown in Fig. 7C, the bands corresponding to Akt and phospho-Akt in NR8383 cells after incubation with 5 mM DM-β-CyD for 24 h were markedly down-regulated, compared with those of control and HP-β-CyD. In addition, DM-β-CyD down-regulated Akt in NR8383 cells as the incubation time with DM-β-CyD increased (Fig. 7D). Furthermore, phosphorylation of Bad, an apoptosis inducible Bcl-2 family protein, was also ameliorated by the treatment with DM-β-CyD (Fig. 7E). These results strongly suggest that DM-β-CyD induces apoptosis through the impairment of activation of PI3K-Akt pathway, not p38 MAPK, followed by the inhibition of phosphorylation of Bad.

3.5. Effects of DM-β-CyD on p53 pathway

The tumor suppressor activity of the p53 protein has been explained by its ability to induce apoptosis in response to a variety of cellular stresses (Fridman and Lowe, 2003). Recent studies have demonstrated that p53 interacts with the pro-apoptotic mitochondrial membrane protein Bak in the induction of apoptosis (Leu et al., 2004). Therefore, to reveal whether p53 is involved in the apoptosis induced by DM-β-CyD, we examined the apoptotic activity of DM-β-CyD in mouse peritoneal macrophages isolated from wild type mice or p53 knockout ($p53^{-/-}$) mice using a flow cytometry after treatment with annexinV-FITC. As shown in Fig. 8, there was no significant difference in the amount of apoptotic cells of peritoneal macrophages between wild type and $p53^{-/-}$ mice. These results suggest that the involvement of p53 in apoptosis induced by DM-β-CyD was only slight.

3.6. Involvement of mitochondria in apoptosis induced by DM-β-CyD

To reveal whether the apoptotic effect of DM-β-CyD is mitochondria-dependent or not, we determined the mitochondrial transmembrane potential using rhodamine 123 after incubation with DM-β-CyD in NR8383 cells (Emaus et al., 1986). The mitochondrial transmembrane potentials of the cells treated with

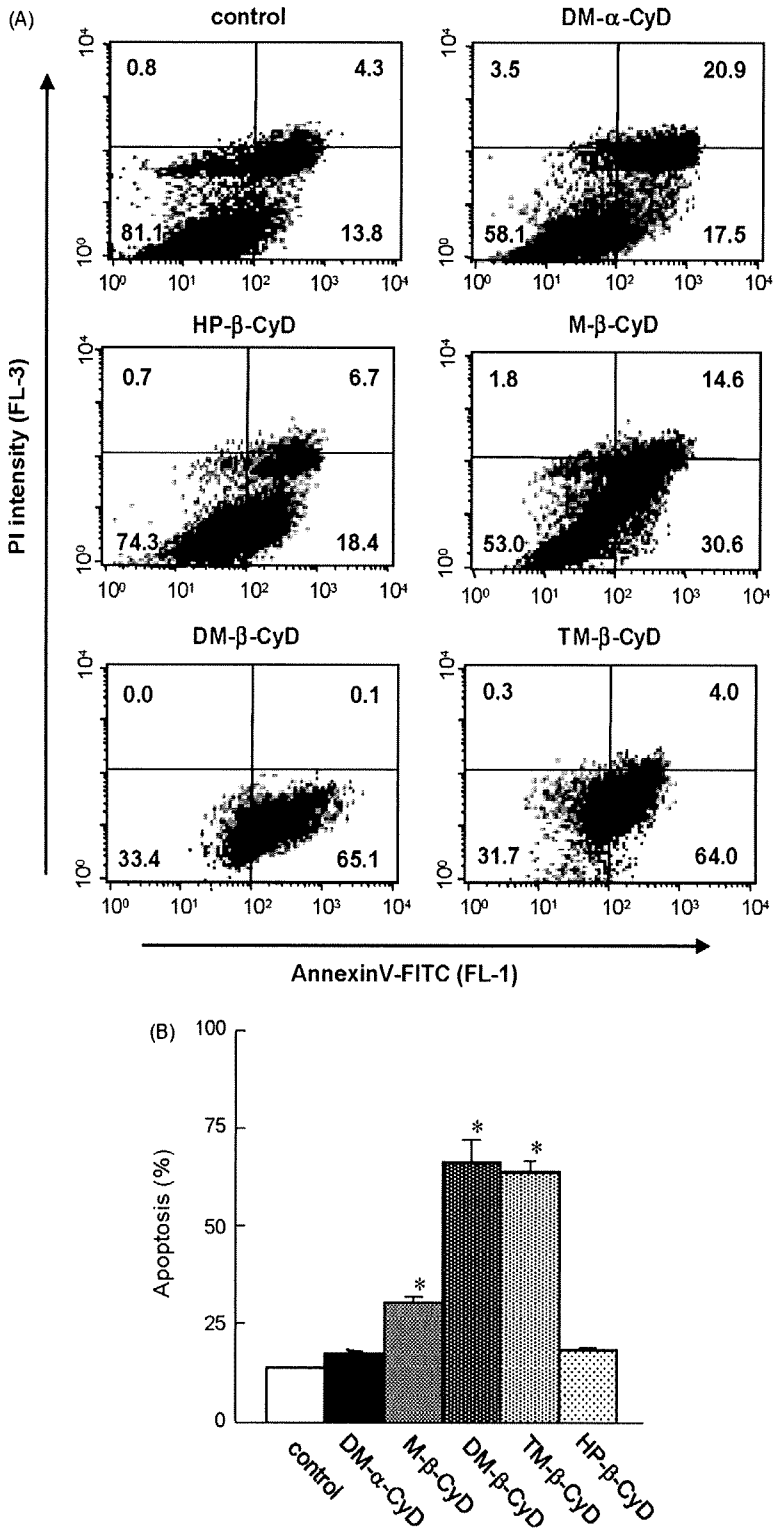

Fig. 5. Effects of CyDs on exposure of PS in NR8383 cells. NR8383 cells were incubated in medium with or without CyDs (5 mM) for 24 h. Then cells were stained with annexinV-FITC and PI, and analyzed using a flow cytometry. (A) Data were plotted as the annexinV-FITC intensity (*X*-axis) *versus* the relative number of PI-positive cells (*Y*-axis). (B) The percentage of cells existing in annexinV-FITC-positive and PI-negative fraction was shown. Each value represents the mean ± S.E.M. of three experiments. *$p < 0.05$ *versus* control.

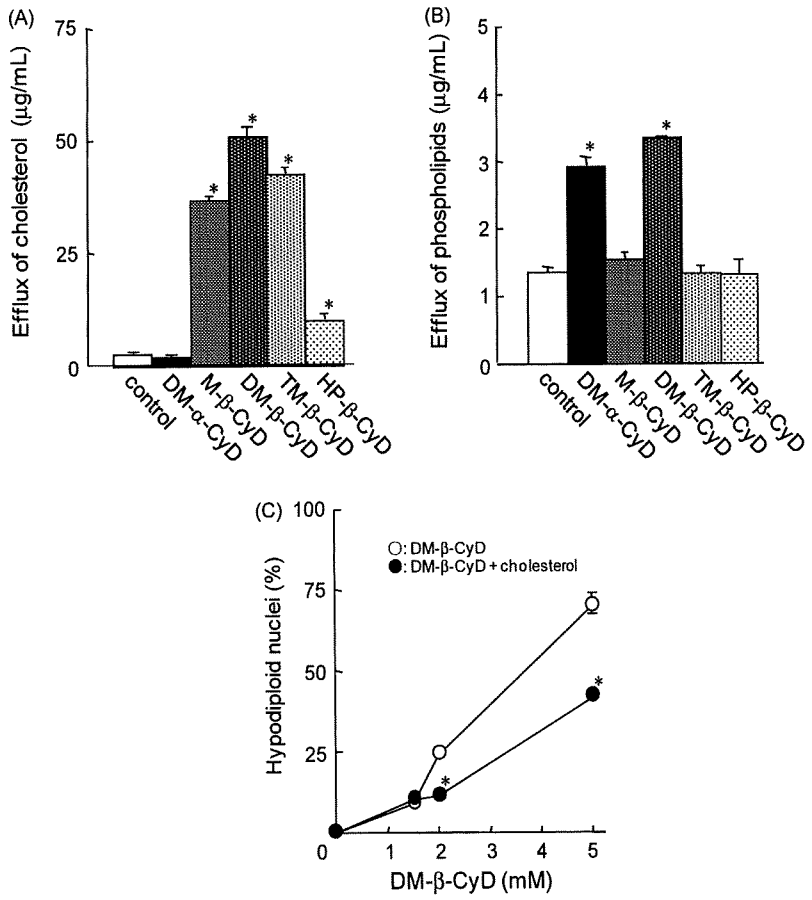

Fig. 6. Effects of CyDs on efflux of cholesterol (A) and phospholipids (B) from NR8383 cells. (A and B) NR8383 cells were incubated in HBSS (pH 7.4) with or without CyDs (5 mM) for 1 h. The concentrations of cholesterol and phospholipids in HBSS were determined by Cholesterol E-test Wako® and Phospholipids C-test Wako®, respectively. Each value represents the mean ± S.E.M. of three experiments. *$p < 0.05$ *versus* control. (C) Effects of cholesterol on apoptosis induced by DM-β-CyD. NR8383 cells were treated with 5 mM DM-β-CyD or cholesterol-loading 5 mM DM-β-CyD for 24 h at 37 °C. After treatment, cells were stained by PI, then the percentage of cells showing DNA degradation was quantified by flow cytometry. Each point represents the mean ± S.E.M. of three experiments. *$p < 0.05$ *versus* DM-β-CyD.

DM-β-CyD and TM-β-CyD were significantly lowered to 1% and 16%, respectively, but those with DM-α-CyD, HP-β-CyD and M-β-CyD decreased to 56%, 87% and 56%, respectively (Fig. 9A and B). It is acknowledged that a decrease in mitochondrial potential leads to the release of cytochrome *c* from mitochondria followed by activation of caspase-9 and caspase-3 through the formation of apoptosome (Wang, 2001). Therefore, we determined the release of cytochrome c from mitochondria after treatment with DM-β-CyD according to the method reported previously (Yang et al., 1997). Successful separation of mitochondrial fractions was validated by determination of cytochrome oxidase IV, a mitochondrial electron transport protein. As shown in Fig. 9C, the only faint band corresponding to cytochrome *c* in mitochondrial fractions of NR8383 cells after treatment with DM-β-CyD was observed, probably due to the release of cytochrome *c* from mitochondria. These results suggest that the apoptosis induced by DM-β-CyD is associated with a mitochondria-dependent pathway.

3.7. Activation of caspase-3 by DM-β-CyD

Caspase cleaves itself or other caspase to convert inactive form (pro-caspase) to active form, and degrade the substrate such as ICAD, PARP (poly(ADP-ribose) polymerase), and actin. Cytochrome *c* is found to activate caspase-9 through binding with Apaf-1, ATP, and pro-casepase-9, results in the activation of caspase-3 (Kroemer and Reed, 2000; Wang, 2001). Therefore, we next examined the effects of DM-β-CyD on caspase-3 activation by Western blot analysis. Treatment of NR8383 cells with DM-β-CyD, not HP-β-CyD, for 24 h, cleaved pro-caspase-3, and then activated caspase-3 (Fig. 10A). Furthermore, the band intensity of actin, one of substrate of capase-3, was decreased by the treatment with DM-β-CyD, not HP-β-CyD, in a time-dependent manner (Fig. 10B). These results suggest that DM-β-CyD induces apoptosis through the activation of caspase-3, resulting from release of cytochrome *c* from mitochondria.

4. Discussion

In the present study, we revealed that of various CyDs, DM-β-CyD potentially caused apoptosis in NR8383, A549 and Jurkat cells, possibly due to cholesterol depletion from cell membranes, and apoptosis induced by DM-β-CyD could result from the inhibition of the activation of PI3K-Akt-Bad pathway, neither p38 MAP kinase nor p53.

Cytotoxicity induced by DM-β-CyD documented herein was found to induce loss of cell viability through apoptotic cell death. The apoptotic character of the cell death was confirmed by the DNA content in nucleus, DNA fragmentation, morphological change, mitochondrial transmembrane potential, cytochrome *c* release from mitochondria, and caspase-3 activation in NR8383 cells. As

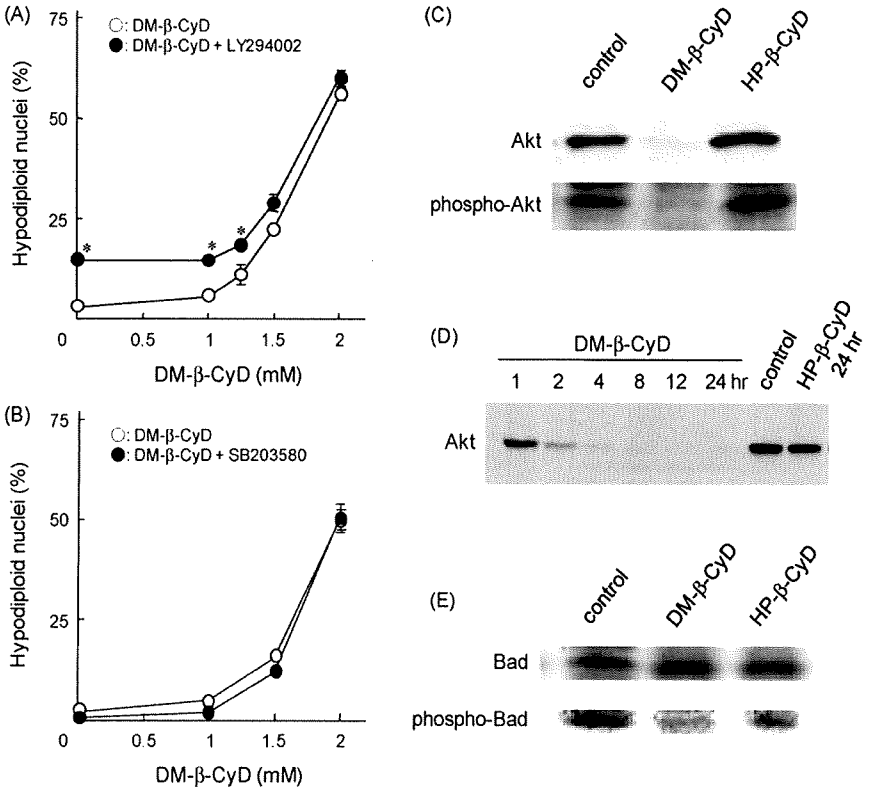

Fig. 7. Effects of PI3K inhibitor (A) and p38 MAP kinase inhibitor (B) on apoptosis induced by DM-β-CyD. Cells were treated with or without LY294002 (10 mM), a PI3K inhibitor for 4 h, or SB203580 (20 mM) for 2 h at 37 °C, and then treated with DM-β-CyD for 24 h at 37 °C. The percentage of cells showing DNA degradation was quantified by flow cytometry after attaining by PI, DM-β-CyD; DM-β-CyD + LY294002 or SB203580. Each point represents the mean ± S.E.M. of three experiments. *$p < 0.05$ *versus* DM-β-CyD. Immunoblot analysis of Akt and phospho-Akt (C and D), Bad and phospho-Bad (E), following treatment with β-CyDs. Cells were treated with 5 mM β-CyDs for 24 h or indicated time at 37 °C.

a whole, these findings strongly suggest that cell death inducted by DM-β-CyD results from apoptosis, not necrosis.

Generally, it is difficult for CyDs to induce apoptosis after uptake into cells, because CyDs have poor membrane permeability due to its aqueous properties and high molecular weight. Therefore, we hypothesized that apoptosis induced by CyDs is involved in the interaction with cell membrane components. Actually, non-ionic surfactants, such as polyethylene glycol sorbitan monolaurate (Tween 20), polyoxyethylenehydrogenated caster oil 60 (HCO-60) and Triton X-100, induced apoptosis in NR8383 cells at more than critical micelle concentrations, probably due to the solubilizing effects of cell membrane components such as cholesterol and phospholipids (data not shown). Therefore, it is highly likely that the solubilizing effects of DM-β-CyD and TM-β-CyD on membrane lipids result in apoptosis, because these methylated β-CyDs have high hemolytic activity through the solubilizing effects on cholesterol (Irie and Uekama, 1997, 1999). However, the possibility that methylated enter cells cannot be ruled out, because methylated CyDs are amphiphilic compounds. Unfortunately, we have no data regarding the membrane permeability of methylated CyDs. Elaborate study is further required for revealing the relationship between apoptotic activity and membrane permeability of methylated CyDs.

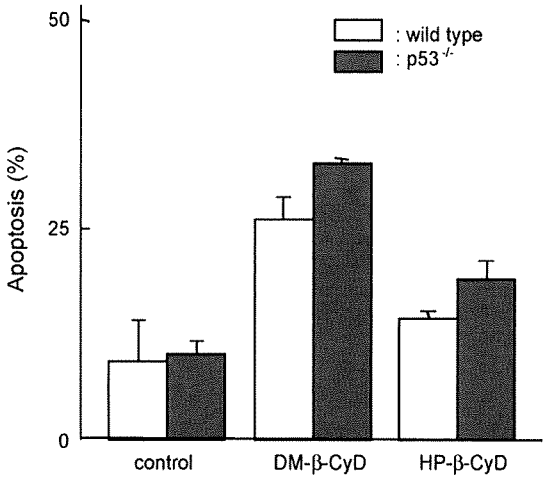

Fig. 8. Effects of β-CyDs on exposure of PS in peritoneal macrophages isolated from wild type or p53-deficient mice. Mouse peritoneal macrophages derived from wild type or $p53^{-/-}$ were treated with β-CyDs (5 mM) for 24 h, and stained with annexinV-FITC and PI, and analyzed using a flow cytometry. Each value represents the mean ± S.E.M. of three experiments.

Recently, it is reported that lipid rafts, which are lipid microdomains mainly composed of cholesterol and sphingolipids, are contributed to apoptosis via FasL/Fas and Bad, an apoptosis inducible factor of Bcl-2 family (Ayllon et al., 2002; Hueber et al., 2002; Legler et al., 2003). In addition, we previously revealed that DM-β-CyD extracted cholesterol from lipid microdomains from Caco-2 cell monolayers (Yunomae et al., 2003). Therefore, we examined whether apoptosis induced by DM-β-CyD is contributed to the extraction of membrane components from lipid rafts. Of various CyDs, M-β-CyD and TM-β-CyD mainly released cholesterol, but DM-α-CyD selectively extracted phospholipids, not cholesterol, while DM-β-CyD released both cholesterol and phospholipids from NR8383 cells (Fig. 6). Of the methylated CyDs, DM-α-CyD did not induce apoptosis even under the experimental conditions where

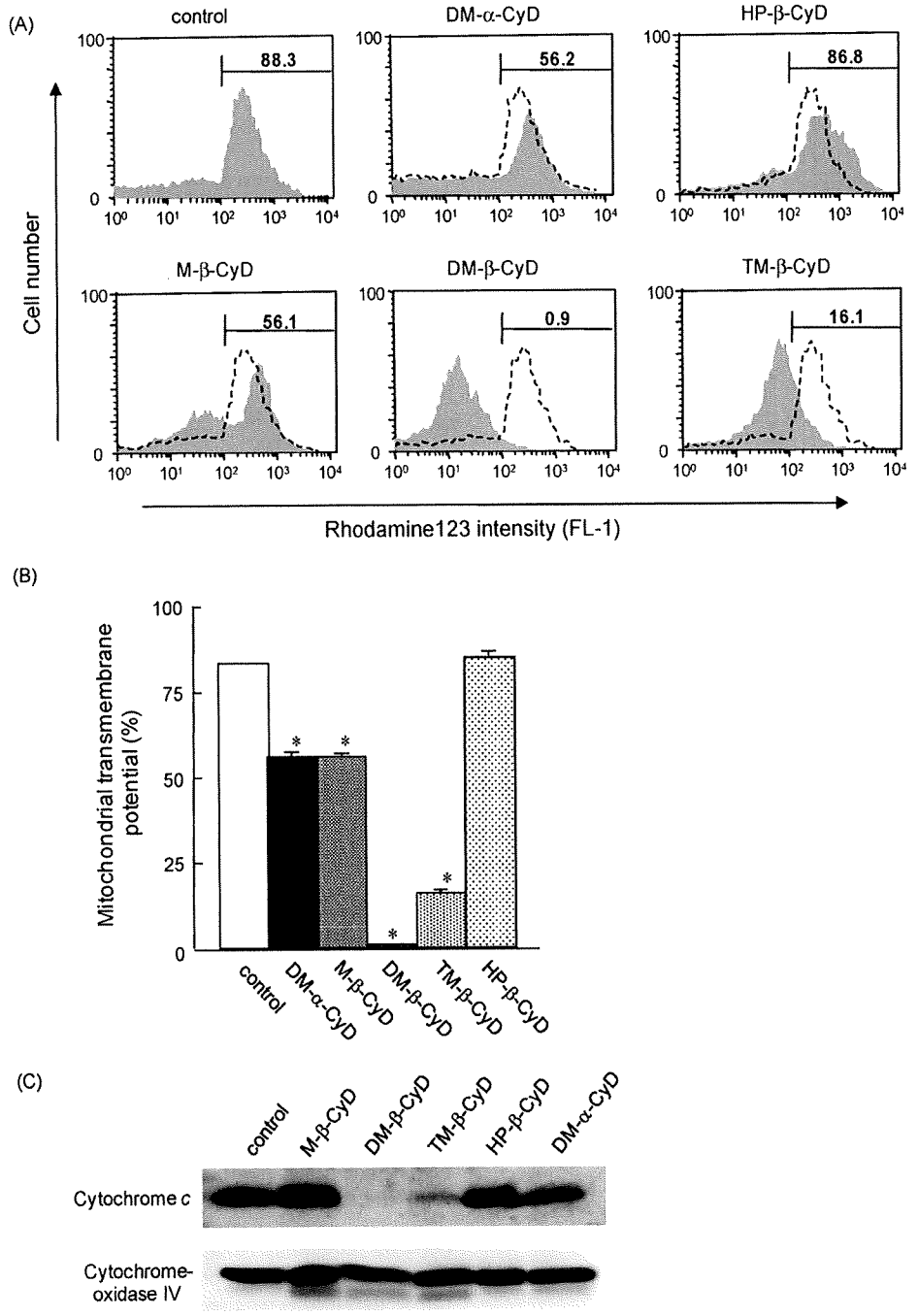

Fig. 9. (A and B) Flow cytometric analysis of mitochondrial transmembrane potential of NR8383 cells treated with CyDs. After incubation with or without CyDs (5 mM) for 24 h, cells were stained with rhodamine 123 and mitochondrial transmembrane potential was analyzed using a flow cytometry. (A) Rhodamine 123 intensity. Dotted line, untreated control and solid line, treated with CyDs. (B) Rate of mitochondrial transmembrane potential (%). Each value represents the mean ± S.E.M. of three experiments. *$p < 0.05$ *versus* control. (C) Immunoblot analysis of cytochrome *c* remaining in mitochondria following treatment of NR8383 cells with CyDs. Cells were treated with 5 mM CyDs for 24 h at 37 °C, mitochondrial fraction was isolated, and cytochrome *c* levels were assayed by Western blot. To verify the purification of mitochondrial fraction, the analysis of cytochrome oxidase IV was also carried out.

cell death was inducted (Figs. 1 and 2). Therefore, we hypothesized that cholesterol depletion in lipid rafts may have a crucial role in the induction of apoptosis by DM-β-CyD. As a result, this hypothesis may be confirmed by the results of cholesterol extraction study and of the rescue study as shown in Fig. 6. However, it remains unclear why M-β-CyD did not induce apoptosis because approximately 60% of cell death was induced under the same experimental conditions (Figs. 1A and 2). Additionally, M-β-CyD released cholesterol from NR8383 cells (Fig. 6A) and induces the same morphological change of RRBC to echinocyte as DM-β-CyD, through the extraction of cholesterol from cholesterol-rich lipid rafts (Motoyama et al., 2009). This unexpected result may be explained by the following reason: the extent of cholesterol released by M-β-CyD may be due to less than the threshold level to induce apoptosis toward NR8383 cells. Further elaborate study to address this reason should be required.

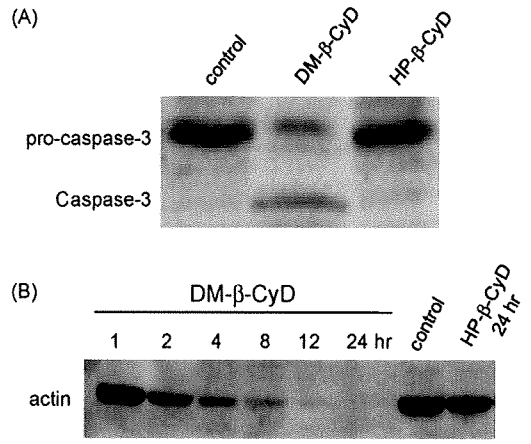

Fig. 10. Immunoblot analysis of caspase-3 (A) and actin (B) following treatment of NR8383 cells with DM-β-CyD. After incubation with 5 mM β-CyDs for 24 h at 37 °C, caspase-3 and actin levels in NR8383 cells were detected by Western blot.

PI3K activates Akt through the recruitment of Akt and PDK1 (3-phospho-inositide-dependent protein kinase-1) to lipid rafts caused by production of $PI(3,4,5)P_3$. This activated-Akt by PI3K suppresses the induction of apoptosis through the phosphorylation of Bad and caspase-9 (Cardone et al., 1998). Therefore, we investigated the effects of PI3K inhibitor (LY294002) on apoptosis induced by DM-β-CyD. The NR8383 cells pretreated with LY294002 showed more potent induction of apoptosis rather than LY294002-untreated cells under the incubation with DM-β-CyD, probably due to the synergistic effects of LY294002 and DM-β-CyD (Fig. 7A). In addition, we revealed that DM-β-CyD significantly suppressed phosphorylation of Akt and accelerated degradation of Akt in NR8383 cells (Fig. 7C and D). These inhibitory effects of DM-β-CyD on activation of Akt may be caused by impairment of recruitment of Akt to lipid rafts through the extraction of cholesterol from lipid rafts. Further study regarding the recruitment of Akt to lipid rafts after treatment with DM-β-CyD should be necessary. Furthermore, we revealed that DM-β-CyD potentially suppressed phosphorylation of Bad (Fig. 7E). Zha et al. reported that suppression of Bad phosphorylation binds with Bcl-x_L, an apoptosis inhibitory factor on mitochondrial cell membrane, resulting in induction of apoptosis (Zha et al., 1996). Therefore, these results strongly suggest the involvement of PI3K-Akt-Bad pathway in apoptosis induced by treatment with DM-β-CyD.

The regulation of p53, a tumor suppressor protein, induces apoptosis through the responses to various stresses such as DNA damage. The p53 protein is primarily regulated at the post-translational level through the ubiquitination-proteasome system, and its ubiquitination is largely induced by MDM2 (a mouse double minute 2). Recently, it is reported that RYBP (RING1 and YY1 binding protein) is a new regulator of the MDM2-p53 loop, and work as a tumor suppressor (Chen et al., 2009). It is also reported that p53 induced apoptosis through the interaction with Bak after translocation of p53 to mitochondria by stress (Leu et al., 2004). Therefore, we investigated whether p53 was involved in the induction of apoptosis by DM-β-CyD using peritoneal macrophages isolated from wild type and $p53^{-/-}$ mice. However, there was no significant difference in the amount of apoptotic cells between wild type and $p53^{-/-}$ mice after treatment with DM-β-CyD (Fig. 8). These results may suggest that the involvement of p53 such as MDM2-p53 loop and p53-Bak interaction in apoptosis induced by DM-β-CyD was only slight.

Signal transduction regarding the induction of apoptosis is largely discriminated into a mitochondrial-dependent or -independent pathway. Mitochondrion have crucial roles in signal transduction of apoptosis, because the activation of caspase family is induced through the reduction of mitochondrial transmembrane potential ($\Delta\psi_m$) following the release of cytochrome *c* prior to apoptosis. DM-β-CyD lowered $\Delta\psi_m$ and induced the release of cytochrome *c* from mitochondria in NR8383 cells (Fig. 9). To release cytochrome *c* from mitochondria during apoptosis, the formation of VDAC (voltage-dependent anion channel) tetramer on the mitochondrial membrane plays an important role (Shimizu et al., 1999, 2001). On the other hand, Bcl-x_L regulates the release of cytochrome *c* through the suppression of VDAC channel activity (Yang et al., 1995; Zha et al., 1996). As apoptosis induction by Bad is contributed to the binding of Bad with Bcl-x_L on the mitochondrial membrane, therefore, the inhibition of phosphorylation of Bad by DM-β-CyD induced the collapse of $\Delta\psi_m$ and released cytochrome *c* from mitochondria (Figs. 7 and 9). Therefore, these results indicate that apoptosis induced by DM-β-CyD is potentially involved in the mitochondria-dependent pathway.

Cytochrome *c* released from mitochondria to cytosol activates caspase-3 through the binding with Apaf-1, ATP and pro-caspase-9 (Kroemer and Reed, 2000; Wang, 2001). In the present study, activated caspase-3 was determined in NR8383 cells treated with DM-β-CyD. In addition, degradation of actin, one of substrate of caspase-3, was observed (Fig. 10). Furthermore, apoptosis induced by DM-β-CyD in Jurkat cells was significantly suppressed by the treatment with z-VAD-fmk, a caspase inhibitor (data not shown). Collectively, these results suggest that activation of caspase-3 is important to induce apoptosis by treatment with DM-β-CyD.

DM-α-CyD may induce necrosis through depletion of sphingomyelin in sphingolipid-rich lipid rafts, because DM-α-CyD did not induce apoptosis in the present study. Actually, our preliminary studies demonstrated that DM-α-CyD released high mobility group box 1 (HMGB1) from NR8383 cells (data not shown), which may support the presumption that DM-α-CyD induces necrotic cell death, because HMGB1 released from cells is known to be a necrosis marker (Tu et al., 2009). In addition, it is well known that ceramide which is synthesized by sphingomyelinase and ceramide synthase is associated with apoptosis, and the decrease in the ceramide or sphingomyelin level in cell membranes may suppress the apoptotic pathway (Pettus et al., 2002). We previously reported that DM-α-CyD released sphingomyelin from sphingolipid-rich lipid rafts of RRBC (Motoyama et al., 2009). Thus, these lines of evidence suggest that disruption of sphingolipid-rich lipid rafts induces necrosis rather than apoptosis toward cells. Taken together, these findings may play a role in a better understanding of the involvement of cholesterol-rich lipid rafts in apoptosis, not sphigolipid-rich lipid rafts. Further elucidation of the apoptotic mechanism involved in cholesterol-rich lipid rafts, not sphingolipid-rich lipid rafts, in various cells may provide insight into the progression and extent of cell death study. Potentially, DM-β-CyD, M-β-CyD and DM-α-CyD may be useful for agents to examine the role of cholesterol-rich lipid rafts and sphingolipid-rich lipid rafts in various events in cells.

Grosse et al. (1998) found that M-β-CyD itself had excellent antitumor activity compared to doxorubicin *in vivo*. After M-β-CyD was administered intraperitoneally during 2 months to Swiss nude mice xenografted with MCF7 or A2789 cells, the antiproliferative activity of M-β-CyD was statistically higher than that of doxorubicin without loosing any body weight. Thus, M-β-CyD is likely to be more preferable to doxorubicin from the viewpoint of both pharmacological and side effects. Considering the findings of the present study, it is possible that DM-β-CyD and TM-β-CyD have the potential to be favorable antitumor agents to M-β-CyD. We are planning to examine the antitumor activity in tumor-bearing mice.

It is important to discuss the safety profiles of parent CyDs, HP-β-CyD and SBE7-β-CyD, because these CyDs are in widespread

clinical use. Parenteral administration of α-CyD and β-CyD, not γ-CyD, has been reported to cause renal toxicity, due to low aqueous solubility and the complexation ability with endogenous lipids, since kidneys is the main organ for the removal of CyDs from systemic circulation and for concentrating CyDs in the proximal convoluted tubule after glomerular filtration (Irie and Uekama, 1997). However, hemolytic activity of parent CyDs is markedly lower than that of methylated CyDs, although the mechanism of hemolysis induced by parent CyD and methylated CyDs is essentially based on the complex formation of CyDs with membrane lipid (Irie and Uekama, 1999). Under the present experimental conditions, α-CyD, β-CyD or γ-CyD did not provide cell death at the concentration of 5 mM in NR8383 cells (Fig. 2B). Thus, it is evident that parent CyDs provide less cytotoxicity than methylated CyDs, although parenteral application of α-CyD and β-CyD should require careful attention. Meanwhile, we demonstrated here that HP-β-CyD had much less cytotoxic activity than methylated CyDs (Figs. 1–10). In addition, HP-β-CyD and SBE7-β-CyD are known to have less hemolytic behavior or less toxic tubular nephritis than β-CyD, because SBE7-β-CyD and HP-β-CyD caused substantially less membrane disruption and are excreted in the urine faster and to a greater extent than β-CyD (Rajewski et al., 1995; Goule and Scott, 2005). Importantly, SBE7-β-CyD has a greatly reduced ability to solubilize cholesterol relative to HP-β-CyD. These lines of evidence suggest that parent CyDs, SBE7-β-CyD and HP-β-CyD have higher safety profile than methylated CyDs.

In conclusion, the present study may demonstrate that DM-β-CyD, not DM-α-CyD, induced apoptosis through the inhibition of the activation of PI3K-Akt-Bad pathway, resulting from cholesterol depletion in lipid rafts of cell membranes. These results will provide useful information for the involvement of various lipid rafts in cell death.

Acknowledgements

This work was partially supported by a Grant-in-Aid from Start-up of Young Scientists from the Ministry of Education, Science and Culture of Japan (20890166).

References

Allen, D.L., Linderman, J.K., Roy, R.R., Bigbee, A.J., Grindeland, R.E., Mukku, V., Edgerton, V.R., 1997. Apoptosis: a mechanism contributing to remodeling of skeletal muscle in response to hindlimb unweighting. Am. J. Physiol. 273, C579–587.

Ashkenazi, A., 2008. Directing cancer cells to self-destruct with pro-apoptotic receptor agonists. Nat. Rev. Drug Discov. 7, 1001–1012.

Ayllon, V., Fleischer, A., Cayla, X., Garcia, A., Rebollo, A., 2002. Segregation of Bad from lipid rafts is implicated in the induction of apoptosis. J. Immunol. 168, 3387–3393.

Bollinger, C.R., Teichgraber, V., Gulbins, E., 2005. Ceramide-enriched membrane domains. Biochim. Biophys. Acta 1746, 284–294.

Brown, D.A., London, E., 1998. Functions of lipid rafts in biological membranes. Annu. Rev. Cell Dev. Biol. 14, 111–136.

Burger, K., Gimpl, G., Fahrenholz, F., 2000. Regulation of receptor function by cholesterol. Cell Mol. Life Sci. 57, 1577–1592.

Cardone, M.H., Roy, N., Stennicke, H.R., Salvesen, G.S., Franke, T.F., Stanbridge, E., Frisch, S., Reed, J.C., 1998. Regulation of cell death protease caspase-9 by phosphorylation. Science 282, 1318–1321.

Chen, D., Zhang, J., Li, M., Rayburn, E.R., Wang, H., Zhang, R., 2009. RYBP stabilizes p53 by modulating MDM2. EMBO Rep. 10, 166–172.

Crowder, C.M., 2009. Cell biology. Ceramides—friend or foe in hypoxia? Science 324, 343–344.

Davis, R.J., 2000. Signal transduction by the JNK group of MAP kinases. Cell 103, 239–252.

Dobrowsky, R.T., 2000. Sphingolipid signalling domains floating on rafts or buried in caves? Cell Signal. 12, 81–90.

Dykstra, M., Cherukuri, A., Sohn, H.W., Tzeng, S.J., Pierce, S.K., 2003. Location is everything: lipid rafts and immune cell signaling. Annu. Rev. Immunol. 21, 457–481.

Edidin, M., 2003. The state of lipid rafts: from model membranes to cells. Annu. Rev. Biophys. Biomol. Struct. 32, 257–283.

Edinger, A.L., Thompson, C.B., 2004. Death by design: apoptosis, necrosis and autophagy. Curr. Opin. Cell Biol. 16, 663–669.

Emaus, R.K., Grunwald, R., Lemasters, J.J., 1986. Rhodamine 123 as a probe of transmembrane potential in isolated rat-liver mitochondria: spectral and metabolic properties. Biochim. Biophys. Acta 850, 436–448.

Fauvelle, F., Debouzy, J.C., Crouzy, S., Goschl, M., Chapron, Y., 1997. Mechanism of α-cyclodextrin-induced hemolysis. 1. The two-step extraction of phosphatidylinositol from the membrane. J. Pharm. Sci. 86, 935–943.

Franke, T.F., Hornik, C.P., Segev, L., Shostak, G.A., Sugimoto, C., 2003. PI3K/Akt and apoptosis: size matters. Oncogene 22, 8983–8998.

Fridman, J.S., Lowe, S.W., 2003. Control of apoptosis by p53. Oncogene 22, 9030–9040.

Gniadecki, R., 2004. Depletion of membrane cholesterol causes ligand-independent activation of Fas and apoptosis. Biochem. Biophys. Res. Commun. 320, 165–169.

Goule, S., Scott, R.C., 2005. 2-Hydroxypropyl-β-cyclodextrin (HP-β-CD): A toxicology review. Food Chem. Toxicol. 43, 1451–1459.

Grassme, H., Schwarz, H., Gulbins, E., 2001. Molecular mechanisms of ceramide-mediated CD95 clustering. Biochem. Biophys. Res. Commun. 284, 1016–1030.

Grosse, P.Y., Bressolle, F., Pinguet, F., 1998. Antiproliferative effect of methyl-β-cyclodextrin in vitro and in human tumour xenografted athymic nude mice. Br. J. Cancer 78, 1165–1169.

Hamasaki, K., Kogure, K., Ohwada, K., 1996. A biological method for the quantitative measurement of tetrodotoxin (TTX): tissue culture bioassay in combination with a water-soluble tetrazolium salt. Toxicon 34, 490–495.

Hueber, A.O., Bernard, A.M., Herincs, Z., Couzinet, A., He, H.T., 2002. An essential role for membrane rafts in the initiation of Fas/CD95-triggered cell death in mouse thymocytes. EMBO Rep. 3, 190–196.

Irie, T., Uekama, K., 1997. Pharmaceutical applications of cyclodextrins. III. Toxicological issues and safety evaluation. J. Pharm. Sci. 86, 147–162.

Irie, T., Uekama, K., 1999. Cyclodextrins in peptide and protein delivery. Adv. Drug Deliv. Rev. 36, 101–123.

Irie, T., Otagiri, M., Sunada, M., Uekama, K., Ohtani, Y., Yamada, Y., Sugiyama, Y., 1982. Cyclodextrin-induced hemolysis and shape changes of human erythrocytes in vitro. J. Pharmacobiodyn. 5, 741–744.

Kabouridis, P.S., Janzen, J., Magee, A.L., Ley, S.C., 2000. Cholesterol depletion disrupts lipid rafts and modulates the activity of multiple signaling pathways in T lymphocytes. Eur. J. Immunol. 30, 954–963.

Kim, R., Emi, M., Tanabe, K., 2005. Caspase-dependent and -independent cell death pathways after DNA damage (review). Oncol. Rep. 14, 595–599.

Kroemer, G., Reed, J.C., 2000. Mitochondrial control of cell death. Nat. Med. 6, 513–519.

Lacour, S., Hammann, A., Grazide, S., Lagadic-Gossmann, D., Athias, A., Sergent, O., Laurent, G., Gambert, P., Solary, E., Dimanche-Boitrel, M.T., 2004. Cisplatin-induced CD95 redistribution into membrane lipid rafts of HT29 human colon cancer cells. Cancer Res. 64, 3593–3598.

Lavrik, I.N., Golks, A., Krammer, P.H., 2005. Caspases: pharmacological manipulation of cell death. J. Clin. Invest. 115, 2665–2672.

Le Roy, C., Wrana, J.L., 2005. Clathrin- and non-clathrin-mediated endocytic regulation of cell signalling. Nat. Rev. Mol. Cell Biol. 6, 112–126.

Legler, D.F., Micheau, O., Doucey, M.A., Tschopp, J., Bron, C., 2003. Recruitment of TNF receptor 1 to lipid rafts is essential for TNFα-mediated NF-κB activation. Immunity 18, 655–664.

Leu, J.I., Dumont, P., Hafey, M., Murphy, M.E., George, D.L., 2004. Mitochondrial p53 activates Bak and causes disruption of a Bak-Mcl1 complex. Nat. Cell Biol. 6, 443–450.

Li, Y.C., Park, M.J., Ye, S.K., Kim, C.W., Kim, Y.N., 2006. Elevated levels of cholesterol-rich lipid rafts in cancer cells are correlated with apoptosis sensitivity induced by cholesterol-depleting agents. Am. J. Pathol., 168, 1107–1118; quiz 1404–1105.

Loos, B., Engelbrecht, A.M., 2009. Cell death: a dynamic response concept. Autophagy, 5.

Mejillano, M., Yamamoto, M., Rozelle, A.L., Sun, H.Q., Wang, X., Yin, H.L., 2001. Regulation of apoptosis by phosphatidylinositol 4,5-bisphosphate inhibition of caspases, and caspase inactivation of phosphatidylinositol phosphate 5-kinases. J. Biol. Chem. 276, 1865–1872.

Motoyama, K., Toyodome, H., Onodera, R., Irie, T., Hirayama, F., Uekama, K., Arima, H., 2009. Involvement of lipid rafts of rabbit red blood cells in morphological changes induced by methylated β-cyclodextrins. Biol. Pharm. Bull. 32, 700–705.

Ohtani, Y., Irie, T., Uekama, K., Fukunaga, K., Pitha, J., 1989. Differential effects of α-, β- and γ-cyclodextrins on human erythrocytes. Eur. J. Biochem. 186, 17–22.

Ono, N., Arima, H., Hirayama, F., Uekama, K., 2001. A moderate interaction of maltosyl-α-cyclodextrin with Caco-2 cells in comparison with the parent cyclodextrin. Biol. Pharm. Bull. 24, 395–402.

Parpal, S., Karlsson, M., Thorn, H., Stralfors, P., 2001. Cholesterol depletion disrupts caveolae and insulin receptor signaling for metabolic control via insulin receptor substrate-1, but not for mitogen-activated protein kinase control. J. Biol. Chem. 276, 9670–9678.

Pettus, B.J., Chalfant, C.E., Hannun, Y.A., 2002. Ceramide in apoptosis: an overview and current perspectives. Biochim. Biophys. Acta 1585, 114–125.

Rajewski, R.A., Traiger, G., Bresnahan, J., Jaberaboansari, P., Stella, V.J., Thompson, D.O., 1995. Preliminary safety evaluation of parenterally administered sulfoalkyl ether b-cyclodextrin derivatives. J. Pharm. Sci. 84, 927–932.

Shimizu, S., Narita, M., Tsujimoto, Y., 1999. Bcl-2 family proteins regulate the release of apoptogenic cytochrome c by the mitochondrial channel VDAC. Nature 399, 483–487.

Shimizu, S., Matsuoka, Y., Shinohara, Y., Yoneda, Y., Tsujimoto, Y., 2001. Essential role of voltage-dependent anion channel in various forms of apoptosis in mammalian cells. J. Cell Biol. 152, 237–250.